

<https://helda.helsinki.fi>

Molecular insights into the function of the viral RNA silencing suppressor HCPro

Ivanov, Konstantin

2016

pöylvanov , K , Eskelin , K J , Baai , M , Swarnalok , D , Lohmus , A , Va
Mäkinen , K M 2016 , ' Molecular insights into the function of the viral RNA silencing
suppressor HCPro ' , Plant Journal , vol. 85 , no. 1 , pp. 30-45 . <https://doi.org/10.1111/tpj.13088>

<http://hdl.handle.net/10138/297740>

<https://doi.org/10.1111/tpj.13088>

cc_by

acceptedVersion

Downloaded from Helda, University of Helsinki institutional repository.

This is an electronic reprint of the original article.

This reprint may differ from the original in pagination and typographic detail.

Please cite the original version.

Molecular insights into the function of the viral RNA silencing suppressor HCPro

Journal:	<i>The Plant Journal</i>
Manuscript ID	TPJ-00775-2015.R1
Manuscript Type:	Original Article
Date Submitted by the Author:	n/a
Complete List of Authors:	Ivanov, Konstantin; University of Helsinki, Food and Environmental Sciences Eskelin, Katri; University of Helsinki, Food and Environmental Sciences Bašić, Marta; University of Helsinki, Food and Environmental Sciences De, Swarnalok; University of Helsinki, Food and Environmental Sciences Lõhmus, Andres; University of Helsinki, Food and Environmental Sciences Varjosalo, Markku; University of Helsinki, Institute of Biotechnology Mäkinen, Kristiina; University of Helsinki, Food and environmental sciences
Key Words:	Potyvirus, HCPro, RNA silencing, silencing supressor, Nicotiana benthamiana, methionin cycle, translational repression, Argonaute, S-adenosyl-L-methionine synthase, S-adenosyl-L-homocysteine hydrolase

SCHOLARONE™
Manuscripts

**Molecular insights into the function of the viral RNA silencing
suppressor HCPro**

Konstantin I. Ivanov^a, Katri Eskelin^{a*}, Marta Bašić^a, Swarnalok De^a, Andres Lõhmus^a, Markku
Varjosalo^b and Kristiina Mäkinen^{a#}

^a Department of Food and Environmental Sciences, Viikki Plant Science Centre, University of
Helsinki, 00014 Helsinki, Finland

^b Institute of Biotechnology, University of Helsinki, 00014 Helsinki, Finland.

[#] Corresponding author: Kristiina Mäkinen, Department of Food and Environmental Sciences,
University of Helsinki, 00014 Helsinki, Finland, tel. +358294158411,
kristiina.makinen@helsinki.fi,

Running title: Mechanisms of RNA silencing suppression by HCPro

Keywords: potyvirus, HCPro, RNA silencing, post-transcriptional gene silencing, silencing
suppressor, methionine cycle, translational repression, Argonaute, S-adenosyl-L-methionine
synthase, S-adenosyl-L-homocysteine hydrolase

Total word count (8656); abstract (199), introduction (819), results (2548), discussion (2730),
experimental procedures (521), acknowledgements (137), figure legends (1702)

* Present address: Department of Biosciences, University of Helsinki, 00014 Helsinki, Finland.

20 ABSTRACT

21 Potyviral HCPro is a well-characterized suppressor of antiviral RNA silencing, but its
22 mechanism of action is not yet fully understood. In this study, we used affinity purification coupled
23 with mass spectrometry to identify binding partners of HCPro in potyvirus-infected plant cells. This
24 approach led to the identification of various HCPro interactors, including two key enzymes of the
25 methionine cycle, S-adenosyl-L-methionine synthase (SAMS) and S-adenosyl-L-homocysteine
26 hydrolase (SAHH). This finding, along with the results of enzymatic activity and gene knockdown
27 experiments, suggests a mechanism in which HCPro complexes containing viral and host proteins
28 act to suppress antiviral RNA silencing through local disruption of the methionine cycle. Another
29 group of HCPro interactors identified in this study represented ribosomal proteins. Immunoaffinity
30 purification of ribosomes demonstrated that HCPro is associated with ribosomes in virus-infected
31 cells. Furthermore, we show that HCPro and AGO1, the core component of the RNA-induced
32 silencing complex (RISC), interact with each other and are both associated with ribosomes *in*
33 *planta*. These results, together with the fact that AGO1 association with ribosomes is a hallmark of
34 RISC-mediated translational repression, suggest a second mechanism of HCPro action, whereby
35 ribosome-associated multiprotein complexes containing HCPro relieve viral RNA translational
36 repression through the interaction with AGO1.

38 SIGNIFICANCE STATEMENT

39 Although HCPro is a well-characterized suppressor of antiviral RNA silencing, its mechanism of
40 action is not fully understood. The results of the present study suggest two putative mechanisms by
41 which potyvirus-specific complexes containing HCPro are involved in suppression of RNA
42 silencing. The first is through local disruption of the methionine cycle to block sRNA methylation.

1
2
3 43 The second mechanism is the relief of viral RNA translational repression by ribosome-associated
4
5 44 multiprotein complexes containing HCPro.
6
7 45
8
9
10 46 INTRODUCTION
11
12
13 47 Potyviruses comprise one of the most widely distributed (Roossinck 2012) and
14
15 48 economically important (Scholthof *et al.* 2011) groups of plant viruses. Their genome is a positive-
16
17 49 sense ssRNA molecule of about 10,000 nucleotides containing two open reading frames (ORFs).
18
19 50 The first large ORF is translated into a single polyprotein, which is processed into individual mature
20
21 51 proteins by viral proteases. The second short ORF (PIPO) is embedded within the P3 cistron of the
22
23 52 polyprotein and translated as the P3-PIPO fusion protein (Chung *et al.* 2008). Like all other viruses,
24
25 53 potyviruses are under constant selection pressure to keep their genomes as compact and optimized
26
27 54 as possible. As a result, potyviral proteins are often multifunctional and the best example of this is
28
29 55 helper component proteinase (HCPro). As its name implies, HCPro is a papain-like cysteine
30
31 56 proteinase responsible for its self-cleavage from the polyprotein precursor (Carrington and Herndon
32
33 57 1992, Verchot *et al.* 1992). Besides its proteolytic function, HCPro is also involved in viral cell-to-
34
35 58 cell and long-distance movement (Rojas *et al.* 1997, Saenz *et al.* 2002), genome replication
36
37 59 (Kasschau and Carrington 1995), aphid transmission (Govier *et al.* 1977, Pirone and Blanc 1996),
38
39 60 symptom development (Redondo *et al.* 2001) and viral synergism (Pruss *et al.* 1997, Shi *et al.* 1997,
40
41 61 Wang *et al.* 2002). Other functions of HCPro include inhibition of the endonuclease (Ballut *et al.*
42
43 62 2005) and protease (Sahana *et al.* 2012) activities of the 20S proteasome and increasing the yield of
44
45 63 viral particles (Valli *et al.* 2014). Furthermore, HCPro interacts with several host factors including
46
47 64 endogenous suppressor of RNA silencing rgs-CaM (Anandalakshmi *et al.* 2000), ethylene-inducible
48
49 65 transcription factor RAV2 (Endres *et al.* 2010), translation initiation factors eIF4E/iso4E (Ala-
50
51 66 Poikela *et al.* 2011), RING-finger protein HIP1 (Guo *et al.* 2003) and microtubule-associated
52
53 67 protein HIP2 (Haikonen *et al.* 2013).
54
55
56
57
58
59
60

Perhaps the most widely known and studied property of HCPro is its ability to suppress RNA silencing (Pruss, *et al.* 1997, Anandalakshmi *et al.* 1998, Brigneti *et al.* 1998, Kasschau and Carrington 1998). However, despite extensive research, the molecular mechanism underlying this ability is not yet fully understood. The prevailing hypothesis is that RNA silencing suppression by HCPro involves direct binding and sequestration of small RNA (sRNA) duplexes (Lakatos *et al.* 2006, Shibolet *et al.* 2007). A possible alternative or complementary mechanism is the inhibition of sRNA methylation (Ebhardt *et al.* 2005, Yu *et al.* 2006, Lozsa *et al.* 2008), leading to sRNA polyuridylation (Li *et al.* 2005) and degradation (Ramachandran and Chen 2008). This could be achieved through HCPro-mediated inhibition of HUA ENHANCER 1 (HEN1), the enzyme responsible for sRNA methylation (Yu *et al.* 2005, Yang *et al.* 2006). HCPro of *Zucchini yellow mosaic virus* (ZYMV) has been reported to physically interact with HEN1 and inhibit its methyltransferase activity *in vitro* (Jamous *et al.* 2011). However, pull-down assays from transgenic plants expressing P1/HCPro of *Turnip mosaic virus* (TuMV) were unable to identify HEN1 as an *in vivo* binding partner of HCPro, arguing against the direct interaction model (Yu, *et al.* 2006). Therefore, we undertook this study to understand how HCPro of *Potato virus A* (PVA) inhibits sRNA methylation and what other mechanisms are involved in the suppression of RNA silencing by HCPro. Our results suggest two distinct but potentially overlapping mechanisms by which HCPro performs its silencing suppressor function. In the first mechanism, HCPro, together with other viral and host proteins, inhibits two key enzymes of the methionine cycle, S-adenosyl-L-methionine synthase (SAMS) and S-adenosyl-L-homocysteine hydrolase (SAHH), depriving HEN1 of its substrate SAM and poisoning HEN1 by its feedback inhibitor SAH. As a result, HEN1 becomes unable to methylate sRNAs, which in turn leads to suppression of RNA silencing. In the second putative mechanism, the ribosome-associated, virus-specific complex containing HCPro, CI and VPg or its precursor VPg-Pro acts to relieve viral RNA translational repression through the interaction with the core RISC component AGO1.

RESULTS

Identification of HCPro binding partners in potyvirus-infected plants

As a first step towards understanding the molecular basis of HCPro function, we sought to identify viral and host proteins associated with HCPro *in vivo* in the context of potyvirus infection. Towards this end, we engineered a recombinant PVA expressing affinity-tagged HCPro as part of the viral polyprotein (Supplementary Table S1). We fused the N-terminus of HCPro to the red fluorescent protein (RFP) and two copies of Strep-tag II, a short peptide of 8 amino acids (WSHPQFEK) (Schmidt and Skerra 2007). The fusion protein, designated HCPro^{(2xStrep)-RFP}, had the advantage of higher affinity for engineered streptavidin (Strep-Tactin) (Voss and Skerra 1997) compared to a similar protein containing only a single Strep-tag, thus allowing more efficient purification of HCPro and its associated binding partners. The affinity purification of HCPro^{(2xStrep)-RFP}-containing complexes was carried out on a Strep-Tactin matrix, followed by protein identification using liquid chromatography-tandem mass spectrometry (LC-MS/MS) (Fig. 1a). This approach allowed us to isolate and characterize protein complexes formed under physiological conditions, at endogenous levels of HCPro expression and in the presence of other viral proteins. The starting material for the purification was a cytoplasmic protein extract from upper leaves of *N. benthamiana* systemically infected with the recombinant PVA expressing HCPro^{(2xStrep)-RFP}. Leaves infected with wild type PVA expressing untagged HCPro were used as a negative control to account for nonspecific binding of viral and host proteins to the affinity matrix. All assays, including controls, were carried out in triplicate and independently analyzed by LC-MS/MS to minimize errors and to ensure the reproducibility of the results.

The efficiency of the purification procedure was initially assessed by SDS-polyacrylamide gel electrophoresis (PAGE) followed by silver staining. The staining revealed a clear difference between the purified samples and the controls (Fig. S1), suggesting that the

purification method was effective in isolating HCPro^{(2xStrep)-RFP} and its associated binding partners. The successful purification was confirmed by Western blotting with anti-RFP antibody, which detected HCPro^{(2xStrep)-RFP} in all three purified samples, but not in the controls (Fig. 1b). Finally, LC-MS/MS analysis identified the bait protein HCPro as the most abundant protein in all purified samples (Table 1). Among other proteins identified by LC-MS/MS, two viral proteins, VPg-Pro and CI, have been previously described as binding partners of HCPro (Guo *et al.* 2001, Yambao *et al.* 2003, Roudet-Tavert *et al.* 2007, Zilian and Maiss 2011). Their identification proved that our approach was suitable for the detection of *bona fide* HCPro interactors. The LC-MS/MS identification of VPg-Pro and CI was also confirmed by Western blotting (Fig. 1c, upper and middle panels). Interestingly, the Western blotting results reproducibly showed that VPg-Pro and CI formed stable high molecular weight complexes with HCPro, which were not fully dissociated during SDS-PAGE.

For the purposes of this study, we focused on two groups of host proteins present in LC-MS/MS data with the bait protein HCPro but not in the purification controls. The first group consisted of several proteins of the large and small ribosomal subunits, suggesting the involvement of HCPro in translational regulation. The association of HCPro with ribosomes was confirmed using an independent ribosome purification method described in a subsequent paragraph. The second group included two key enzymes of the methionine cycle, S-adenosyl-L-methionine synthase 1 (SAMS1, SAM1, MAT1) and S-adenosyl-L-homocysteine hydrolase (SAHH, AdoHcyase) (see Table 1). Until now, only the interaction of HCPro with SAHH, but not SAMS, has been described in the literature (Canizares *et al.* 2013). Therefore, we confirmed that SAMS can be specifically co-precipitated with HCPro^{(2xStrep)-RFP} by Western blotting with anti-SAMS1 antibody. (Fig. 1c, lower panel). The Western blot analysis also revealed that SAMS formed stable high molecular weight complexes with HCPro, similarly to VPg-Pro and CI (Fig. 2).

PVA infection inhibits SAMS enzymatic activity in an HCPro-dependent manner

Having shown that SAMS can be specifically co-purified with HCPro, we next sought to investigate whether PVA infection would affect the enzymatic reaction of SAM synthesis catalyzed by SAMS. We employed a well-established method for measuring SAMS activity based on quantification of radioactivity incorporated into SAM during its synthesis from ³⁵S-labeled methionine (Met) and ATP. In this method, the SAM synthesis reaction is followed by separation of the newly formed SAM from the unreacted ³⁵S-Met and quantification of the radioactivity incorporated into SAM by liquid scintillation counting (Shen *et al.* 2002). Using this experimental approach, we measured total SAMS activity in soluble protein extracts from leaves of PVA-infected *N. benthamiana* plants at 5 days post infection (dpi) with an *Agrobacterium* strain carrying PVA cDNA (Supplementary Table S1). To account for nonspecific effects of agroinfiltration, control plants were infiltrated with the same amount of *Agrobacterium* carrying a vector constitutively expressing an irrelevant β -glucuronidase (*GUS*) gene. The results shown in Fig. 3a demonstrate that SAMS activity was decreased in PVA-infected plants compared to control plants. The decrease was not due to SAMS degradation, since similar SAMS protein levels were observed in mock- and PVA-infected plants (Fig. 3b). To determine whether the inhibitory effect was HCPro-dependent, we constructed a mutant virus lacking HCPro (PVA Δ HCPro; Supplementary Table S1) and compared its ability to inhibit SAMS activity with that of the wild type virus. We observed that the loss of HCPro restored SAMS-mediated catalysis close to its normal levels (Fig. 3a). One possible interpretation of this result is that the effect of PVA infection on SAMS activity is dependent on the presence of HCPro sequence in the viral genome. However, expression of HCPro alone was not sufficient to inhibit the enzymatic activity of SAMS (Fig. S3), suggesting that the inhibition requires HCPro cooperation with other viral proteins or an HCPro-dependent viral process. Collectively, our results suggest that during potyvirus infection, HCPro acts together with other viral proteins to inhibit SAM synthesis, one of the most critical steps in the methionine cycle.

Knockdown of *SAMS*, *SAHH* and *HEN1* partially rescues the HCPro-deficient virus phenotype

Based on the above findings, we hypothesized that successful potyvirus infection requires HCPro-dependent inhibition of the methionine cycle. If this hypothesis were true, transient silencing of *SAMS* and *SAHH* would compensate for the loss of HCPro and rescue the HCPro-deficient virus phenotype. To test this possibility, we generated knockdown constructs expressing intron-spliced hairpin RNAs targeting *SAMS* and *SAHH*. Each construct was designed to target all known members of the corresponding gene family. The constructs were transformed into *Agrobacterium* and co-infiltrated into *N. benthamiana* leaves together with *Agrobacterium* strains harboring PVA Δ HCPro and a control reporter vector expressing Firefly luciferase (Fluc^{int}), which was used to account for virus-nonspecific effects of the knockdown. Because PVA Δ HCPro has been engineered to express *Renilla* luciferase (Rluc; see Supplementary Table S1), we were able to assess viral gene expression by measuring Rluc activity. Control plants were infiltrated with the same amount of *Agrobacterium* harboring PVA Δ HCPro, Fluc^{int} and an empty silencing vector lacking any hairpin RNA sequence. In order to quantify viral gene expression, Rluc activity was measured at 5 dpi and normalized to the corresponding Fluc internal control. Fig. 4a shows that the normalized viral gene expression was increased in cells infected with HCPro-deficient PVA following the knockdown of *SAMS* or *SAHH*. Furthermore, a synergistic effect was observed when both genes were knocked down simultaneously. It is worth noting that the simultaneous down-regulation of *SAMS* and *SAHH* had a stronger effect on various cellular methylation-dependent processes than their individual knockdown, which manifested itself by overpowering any positive effects on Fluc expression (Fig. S4). However, despite the inhibitory effect on Fluc expression, the virus-driven Rluc expression was not similarly affected (Fig. S4), highlighting the virus-specific effect of the knockdown. These results allowed us to conclude that the knockdown of *SAMS* and

SAHH can rescue, albeit only partially (Fig. S5), the defective PVA phenotype associated with the loss of HCPro. This, in turn, supports the hypothesis that one of the functions of HCPro during potyvirus infection is to inhibit SAMS and SAHH, disrupting the methionine cycle. Interestingly, the copy number of PVA Δ HCPro RNA was higher in cells with downregulated *SAMS* or *SAHH* and increased even further when both genes were knocked down simultaneously (Fig. 4b). This result indicated that the inhibition of SAMS and SAHH led to viral RNA stabilization and accumulation.

SAM, synthesized by SAMS, serves as a methyl donor for cellular methyltransferases including HEN1. sRNA duplexes formed during RNA silencing are protected from degradation through the 2'-O-methylation of their 3' ends by HEN1 (Yu, *et al.* 2005). We next asked if the partial rescue of PVA Δ HCPro gene expression and RNA accumulation during SAMS and SAHH knockdown was due to reduced HEN1 activity. Fig. 4c shows that the knockdown of *HEN1* increased normalized viral gene expression in cells infected with HCPro-deficient PVA. These data support a hypothesis that HCPro inhibits SAMS and SAHH activity to interfere with sRNA methylation by HEN1, which in turn leads to enhanced sRNA degradation, reduced RNA silencing and increased viral gene expression and accumulation of viral RNA.

HCPro, CI and VPg are associated with ribosomes in infected cells

The finding that HCPro co-purified with several ribosomal proteins prompted us to investigate whether HCPro is associated with ribosomes in PVA-infected cells. Towards this end, we employed immunoaffinity purification of ribosomes via FLAG-tag (Fig. 5a), which proved to be highly effective for isolating ribosomes from *A. thaliana* (Zanetti *et al.* 2005, Mustroph *et al.* 2009, Hummel *et al.* 2012). In order to purify ribosomes from *N. benthamiana*, we used transgenic *N. benthamiana* plants expressing the FLAG-tagged *A. thaliana* ribosomal protein L18B (RPL18B), which can be successfully incorporated into heterologous ribosomes (Pitkanen *et al.* 2014). The

1
2
3 219 FLAG-tagged ribosomes were purified from soluble plant extracts using an anti-FLAG affinity
4
5 220 matrix and the purified samples were analyzed by SDS-PAGE followed by silver staining. Bands of
6
7 221 low molecular mass characteristic of ribosomal proteins (Barakat *et al.* 2001, Chang *et al.* 2005)
8
9 222 were detected in samples purified from transgenic plants (Fig. 5b, left panel), whereas virtually no
10
11 223 such bands were detected in control purifications from non-transgenic plants. Western blotting with
12
13 224 anti-FLAG antibody confirmed that the FLAG-tagged bait protein RPL18B was enriched in the
14
15 225 purified samples (Fig. 5b, right panel). In order to assess the integrity of the purified ribosomes, we
16
17 226 compared RNA isolated from the purified samples with total RNA from *N. benthamiana* leaves,
18
19 227 which is mainly composed of ribosomal RNA (rRNA). The comparison revealed that the purified
20
21 228 samples contained intact rRNA of both ribosomal subunits and that the ratio between 26S and 18S
22
23 229 rRNA was similar to that found in the total RNA sample (Fig. 5c). From these findings, we
24
25 230 concluded that the FLAG tag-based immunoaffinity purification yielded ribosomes of high purity
26
27 231 and integrity. This conclusion was further supported by the results of LC-MS/MS analysis of the
28
29 232 purified ribosomes, which identified 76 out of 80 (95%) ribosomal proteins including the FLAG-
30
31 233 tagged bait protein (Eskelin, Varjosalo and Mäkinen, *personal communication*). As the next step,
32
33 234 we performed immunoaffinity purification of ribosomes from PVA-infected plants. For this
34
35 235 purpose, leaves of transgenic *N. benthamiana* plants expressing FLAG-tagged RPL18B were
36
37 236 infiltrated with an *Agrobacterium* strain carrying PVA cDNA. FLAG-tagged ribosomes were
38
39 237 immunopurified from soluble extracts of PVA-infected transgenic plants and the purified samples
40
41 238 were analyzed by LC-MS/MS. The analysis identified HCPro, CI and VPg as ribosome-associated
42
43 239 viral proteins (Table 2 and Fig. 5a), with VPg being less abundant in the ribosome-associated
44
45 240 complexes than HCPro and CI. None of these proteins was identified in control purifications from
46
47 241 PVA-infected non-transgenic plants, confirming the specificity of the observed interactions. The
48
49 242 association of HCPro and CI with ribosomes was verified by Western blotting (Fig. S8). We could
50
51 243 not detect VPg on the blots, probably due to insufficient sensitivity of the anti-VPg antibody.
52
53
54
55
56
57
58
59
60

However, the established role of VPg in potyviral RNA translation (Eskelin et al., 2011) supports the notion that VPg is a *bona fide* ribosome-associated protein, which is present in ribosomes in much lower amounts than HCPro and CI. These results, together with those of HCPro affinity purification experiments, indicate that HCPro and several other potyviral proteins form virus-specific complexes associated with ribosomes in infected cells.

HCPro forms stable complexes with AGO1

The association of the RNA silencing suppressor HCPro with ribosomes led us to investigate whether HCPro may interact with the core component of the RNA silencing pathway ARGONAUTE1 (AGO1), which binds to ribosomes to repress translation (Lanet *et al.* 2009). As a first step, we examined if AGO1 fused to cyan fluorescent protein (AGO1^{CFP}) could interact with HCPro when both proteins were transiently expressed in *N. benthamiana*. Consistent with previous observations (Chiu *et al.* 2010), expression of AGO1^{CFP} was strongly upregulated in the presence of HCPro, confirming that the transiently expressed HCPro was correctly folded and functionally active (Fig. 6a). Furthermore, HCPro and AGO1^{CFP} formed high molecular weight complexes that were stable enough not to be completely dissociated during SDS-PAGE (Fig. 6a, asterisks). Similar complexes were formed when HCPro was expressed as part of the PVA polyprotein from viral cDNA. No bands corresponding to the HCPro-AGO1^{CFP} complexes were detected in negative controls, which included AGO1^{CFP} co-expression with an irrelevant protein or with PVA lacking HCPro, confirming the specificity of the binding (see Fig. S6 for overexposed image of the Western blot from Fig. 6a). We next determined whether endogenously expressed AGO1 could interact with HCPro in the context of potyvirus infection. For this purpose, we performed Western blot analysis of the protein complexes that co-purified with HCPro^{(2xStrep)-RFP} (see the first paragraph) using an antibody raised against the N-terminal peptide of *A. thaliana* AGO1. In a series of preliminary experiments, we have confirmed that the antibody could also recognize AGO1 from *N.*

benthamiana, albeit with lower sensitivity (Fig. S7). The Western blot analysis showed that the anti-AGO1 antibody recognized high molecular weight complexes in the affinity-purified samples (Figs. 2 and 6b), but not in the negative controls, suggesting that AGO1 was co-purified in a complex with HCPro. Based on the above results, we concluded that HCPro could form stable complexes with AGO1 both when transiently expressed and when expressed from the viral genome *in planta*.

HCPro and AGO1 are both associated with ribosomes

Having shown that HCPro interacts with AGO1, we next asked whether these two proteins could associate with ribosomes in living cells. In order to answer this question, we employed a two-step purification procedure to isolate highly purified ribosomes from the FLAG-RPL18B transgenic plants transiently expressing HCPro^{RFP} and AGO1^{CFP}. The procedure combined a classical method of ultracentrifugation in a continuous sucrose gradient, which has been successfully used to demonstrate the association of AGO1 with ribosomes (Lanet, *et al.* 2009), with the FLAG-tagged ribosome purification (Fig. 6c). Western blot analysis confirmed the successful purification of ribosomes, as evidenced by the detection of FLAG-RPL18B in the purified samples, and showed that the ribosome preparations contained both HCPro^{RFP} and AGO1^{CFP} (Fig. 6c, upper right panels). The two proteins were again detected in large and stable complexes that were not fully dissociated during SDS-PAGE (Fig. 6c, asterisks). To determine whether HCPro and AGO1 can coexist in the same ribosome-associated complexes, we purified ribosomes from the FLAG-RPL18B transgenic plants infected with PVA expressing HCPro^{(2xStrep)-RFP} and analyzed the obtained ribosome preparations for the presence of HCPro^{(2xStrep)-RFP} and endogenous AGO1 by Western blotting. As shown in Fig. S8, protein bands with similar electrophoretic mobility were recognized by both antibodies suggesting the existence of ribosome-associated multiprotein complexes containing both HCPro and AGO1.

1
2
3
4
5
6
7
8
9
10
11
12
13
14
15
16
17
18
19
20
21
22
23
24
25
26
27
28
29
30
31
32
33
34
35
36
37
38
39
40
41
42
43
44
45
46
47
48
49
50
51
52
53
54
55
56
57
58
59
60

DISCUSSION

The purpose of the present study was to investigate molecular mechanisms underlying the ability of HCPro to suppress antiviral RNA silencing in the host cell. At the heart of antiviral RNA silencing are small RNA (sRNA) molecules, typically of 21-24 nucleotides in length, derived from imperfectly base-paired viral RNA hairpins or viral double-stranded RNA (dsRNA) replication intermediates. A similar mechanism regulates host gene expression through endogenously produced sRNA. One source of endogenous sRNA is imperfect hairpins in the transcripts of non-coding micro RNA (miRNA) genes. Another source is transcription of inverted repeats, convergent transcription or the action of cellular RNA-dependent RNA polymerases (reviewed in Bologna and Voinnet 2014). The RNA silencing pathway can be superficially divided into two major stages: the initiation stage involving sRNA biogenesis and the effector stage centered on target gene repression. In the initiation stage, Dicer-like (DCL) endoribonucleases cleave endogenous or exogenous dsRNA precursors into small RNA duplexes. The sRNA duplexes are then protected from degradation through the 2'-O-methylation of their 3' ends by the methyltransferase HEN1 (Yu, *et al.* 2005). Like most methyltransferases, HEN1 uses an endogenous organic molecule, S-adenosyl-L-methionine (SAM, AdoMet), as the methyl group donor. Therefore, the availability of SAM is critical for the methyltransferase activity of HEN1 and, consequently, for the successful initiation of RNA silencing. Another molecule important for the methyltransferase activity of HEN1 is S-adenosyl-L-homocysteine (SAH, AdoHcy), which is a byproduct and a feedback inhibitor of most biological methylation reactions (Clarke and Banfield 2001). SAM and SAH, aside from being the substrate and product of methylation reactions, also represent essential components of the methionine cycle (Fig. 7a). In this cycle, L-methionine is converted to SAM with the help of an enzyme called S-adenosyl-L-methionine synthase (SAMS, MAT). SAM subsequently serves as a methyl donor for cellular methyltransferases, such as HEN1.

The methylation reaction byproduct SAH is subsequently broken down to adenosine and L-homocysteine by an enzyme called S-adenosyl-L-homocysteine hydrolase (SAHH). Finally, L-homocysteine is recycled back to L-methionine by methionine synthase (MS), thus closing the cycle. As can be seen from the above description, the methionine cycle continuously supplies SAM to HEN1 and therefore plays a critical role in the RNA silencing pathway.

In order to overcome antiviral silencing, plant viruses have evolved an arsenal of proteins called RNA silencing suppressors that inhibit various stages of the silencing pathway (reviewed in Pumplin and Voinnet 2013). Despite the fact that HCPro was the first viral RNA silencing suppressor to be discovered (Pruss, *et al.* 1997, Anandalakshmi, *et al.* 1998, Brigneti, *et al.* 1998, Kasschau and Carrington 1998), its mechanism of action is still not fully understood. In this study, we demonstrate that HCPro interacts with two key enzymes of the methionine cycle, SAMS and SAHH. Furthermore, we provide evidence suggesting that PVA infection inhibits the catalytic activity of SAMS in an HCPro-dependent manner. The inhibition occurred only when HCPro was expressed as part of the viral polyprotein, but not when expressed alone, suggesting the involvement of additional viral proteins or HCPro-dependent processes. Finally, we demonstrate that knockdown of SAMS and SAHH acts similarly to knockdown of HEN1 to partially rescue the defective virus phenotype associated with the loss of HCPro and trigger the accumulation of viral RNA. Collectively, these results suggest that HCPro acts together with other viral proteins to disrupt the methionine cycle in the infected cell through the inhibition of its two key enzymes, SAMS and SAHH. We propose a model (Fig. 7b), in which the HCPro-mediated inhibition of SAMS leads to reduced synthesis of the HEN1 substrate SAM. As a result, the substrate-deprived HEN1 is unable to methylate sRNAs, which leads to the inhibition of the antiviral RNA silencing pathway through 3' polyuridylation (Li, *et al.* 2005) and degradation (Ramachandran and Chen 2008) of unmethylated sRNAs. The effect is further enhanced by the inhibition of SAHH, causing the accumulation of the HEN1 inhibitor SAH (Horwich *et al.* 2007). According to the above model,

1
2
3 344 exogenous expression of HCPro would result in the decreased sRNA methylation and,
4
5 345 consequently, in lower sRNA accumulation. Indeed, the decrease in sRNA methylation has been
6
7 346 observed in transgenic plants expressing P1/HCPro of TuMV (Yu, *et al.* 2006) and the reduced
8
9 347 sRNA accumulation has been reported in transgenic plants expressing HCPro of *Tobacco etch virus*
10
11 348 (TEV) (Mallory *et al.* 2001). Interestingly, transgenic expression of TEV HCPro did not interfere
12
13 349 with DNA methylation in the nucleus, suggesting that the nuclear pool of SAMS (Reytor *et al.*
14
15 350 2009) and SAHH (Lee *et al.* 2012) is not inhibited by HCPro and that the inhibition occurs locally
16
17 351 rather than globally. This possibility is also supported by the fact that the knockdown of SAMS and
18
19 352 SAHH had a different effect on the expression of virus-derived Rluc and plasmid-derived Fluc
20
21 353 (Figs. 3a and S4). Therefore, it can be hypothesized that the HEN1 deprivation of SAM and
22
23 354 poisoning by SAH occurs predominantly in virus-induced cytoplasmic compartments where SAMS
24
25 355 and SAHH are sequestered in a complex with HCPro and other viral proteins. The idea that HCPro
26
27 356 acts through the inhibition of the methionine cycle to suppress RNA silencing is also supported by
28
29 357 the findings of Cañizares *et al.* (2013), who have reported that SAHH interacts with HCPro of
30
31 358 *Potato virus Y* (PVY) and that down-regulation of SAHH decreases sRNA accumulation and
32
33 359 suppresses local silencing. As a final remark, it is worth noting that although HEN1 is the most
34
35 360 obvious target for the HCPro-mediated inhibition via the methionine cycle, it is possible that other
36
37 361 cellular methyltransferases are inhibited by the same mechanism. Future studies should attempt to
38
39 362 determine whether this is indeed the case and if so, how the inhibition of these enzymes may affect
40
41 363 host antiviral responses.

42
43
44
45
46
47 364 In the effector stage of RNA silencing, the Dicer-processed sRNA duplexes are
48
49 365 recognized by one of several Argonaute (AGO) proteins. Upon AGO-catalyzed unwinding of the
50
51 366 sRNA duplexes, one of the duplex strands is discarded and another strand is retained by AGO to
52
53 367 form the functional RNA-induced silencing complex (RISC). RISC then uses this “guide” strand to
54
55 368 find partially or fully complementary mRNAs and down-regulate their expression. This is achieved
56
57
58
59
60

by two mechanisms: translational repression, which may be coupled to accelerated target mRNA decay, and endonucleolytic mRNA cleavage, also known as “slicing”. The degree of complementarity between sRNA and its target mRNA has been suggested to determine whether the mRNA will be repressed or cleaved (Hutvagner and Zamore 2002). In animals, where imperfect base pairing with central mismatches in the miRNA-mRNA hybrids is common, translational repression is considered to be the default silencing mechanism. In plants, however, the majority of sRNAs are highly complementary to their targets, and mRNA cleavage has traditionally been viewed as the predominant mechanism of RISC action (Jones-Rhoades *et al.* 2006). In the last few years, this paradigm has been challenged by increasing experimental evidence showing that the RISC-mediated translational repression is as widespread in plants as it is in animals (Brodersen *et al.* 2008). Similar to the situation in animals, the RISC-mediated translational repression in plants involves the association of sRNAs, their mRNA targets and argonaute proteins with ribosomes (Lanet, *et al.* 2009, Reynoso *et al.* 2012). However, the molecular mechanism underlying translational repression in plants only partially overlaps with that of animals (Iwakawa and Tomari 2013), and its plant-specific aspects are schematically represented in Figure 8 (panels a-b).

Considering that translational repression by endogenous miRNAs is common and widespread in plants, it would be logical to assume that a similar mechanism may be employed in plant defense against viruses, i.e. in sRNA-directed antiviral silencing. Indeed, recent evidence has shown that the cap-independent translation of heterologous RNA fused to the 5' internal ribosome entry site (IRES) of TEV can be strongly repressed by small RNA with perfect complementarity to a target sequence in the 5' untranslated region (UTR) or the open reading frame (ORF) (Iwakawa and Tomari 2013). Importantly, the IRES-mediated translation was refractory to “animal-like” translational repression via the 3' UTR target sequences, suggesting a repression mechanism different from the one acting in animals. This alternative mechanism is thought to operate through steric hindrance of ribosome recruitment or movement by the AGO1-containing RISC (Iwakawa

1
2
3
4
5
6
7
8
9
10
11
12
13
14
15
16
17
18
19
20
21
22
23
24
25
26
27
28
29
30
31
32
33
34
35
36
37
38
39
40
41
42
43
44
45
46
47
48
49
50
51
52
53
54
55
56
57
58
59
60

and Tomari 2013) (Fig. 8 a,b). At the cellular level, the AGO1-mediated translational repression of miRNA targets occurs in association with the endoplasmic reticulum (ER) (Li *et al.* 2013). Because potyviruses translate their genomes on ER membranes (Wei *et al.* 2010), the fact that translational repression occurs within the same subcellular compartment further supports the possibility that translational repression represents a means for the host to inhibit viral protein synthesis.

Based on the above arguments, it is reasonable to suggest that the sRNA-mediated translational repression acts as an antiviral defense mechanism in plants. Consequently, the existence of such a mechanism may have driven potyviruses to evolve effective countermeasures in a never-ending molecular “arms race” with the host. The results of the present study suggest that the potyviral RNA silencing suppressor HCPro may play a role in implementing such countermeasures. We employed HCPro affinity purification coupled with mass spectrometry to show that HCPro interacts with ribosomal proteins in potyvirus-infected plants. Immunoaffinity purification of FLAG-tagged ribosomes from infected plants confirmed the ribosomal association of HCPro. Finally, we have demonstrated that HCPro and AGO1, the core component of RISC, interact with each other and are both associated with ribosomes *in planta*. These results, together with the fact that AGO1 association with ribosomes is a hallmark of translational repression (Lanet, *et al.* 2009), suggest a possibility that HCPro acts as an RNA silencing suppressor, at least in part, by relieving translational repression. It is also worth noting that, in addition to the proposed role of AGO1 in potyviral RNA translational repression (Iwakawa and Tomari 2013), other members of the Argonaute family are involved in host defense against potyviruses (Garcia-Ruiz *et al.* 2015). Of these, AGO2 provides a prominent antiviral role in leaves. The mutual relationship between AGO1 and AGO2 in potyviral RNA silencing requires further investigation. Interestingly, HCPro has recently been shown to have an inhibitory effect on translation of naked RNAs in a wheat germ-based *in vitro* translation system (Martinez and Daros 2014). This finding supports the results of the present study, confirming the interaction of HCPro with ribosomes. On the other hand, it does not

contradict our hypothesis that HCPro may assist the relief of sRNA-mediated translational repression because the *in vitro* translation system used by Martínez and Daròs (2014) lacked the necessary biochemical and cellular components of a functioning RNA silencing pathway.

Immunoaffinity purification of FLAG-tagged ribosomes coupled with mass spectrometry revealed that, in addition to HCPro, two other viral proteins, CI and putatively VPg (or its precursor VPg-Pro), are associated with ribosomes in infected plants. These two viral proteins were also identified in the present study as binding partners of HCPro, which is in agreement with literature data showing that HCPro interacts with CI (Guo, *et al.* 2001, Zilian and Maiss 2011) and VPg (Guo, *et al.* 2001, Yambao, *et al.* 2003, Roudet-Tavert, *et al.* 2007). Western blotting analysis demonstrated that HCPro, CI and VPg-Pro formed large multiprotein complexes in infected cells. It could be hypothesized that these complexes associate with ribosomes to help the virus overcome host translational repression and promote translation of its own RNA. In the light of this hypothesis, one can more readily interpret some of the results reported in the literature. For example, it is well established that potyviral VPg interacts with eIF4E and its plant-specific isoform eIF(iso)4E and this interaction is a major determinant of recessive virus resistance (reviewed in Robaglia and Caranta 2006, Truniger and Aranda 2009, Wang and Krishnaswamy 2012). However, the physiological relevance of the interaction between the 5'-terminal VPg and eIF4E/iso4E is not immediately obvious, because potyviral RNA translation proceeds in a cap-independent manner from a downstream IRES and does not require eIF4E for initiation (Gallie 2001, Iwakawa and Tomari 2013). On the other hand, eIF4E is the part of the eIF4F initiation complex, which has been implicated in the sRNA-mediated translational repression (reviewed in Fabian *et al.* 2010). Therefore, it might be possible that the interaction of potyviral VPg with eIF4E may assist the relief of viral RNA translational repression. Indirect support for this possibility comes from the observation that VPg alone functions as a weak RNA silencing suppressor (Rajamaki and Valkonen 2009). Furthermore, consistent with the hypothesis that the ribosome-associated complexes

1
2
3 444 containing VPg or its precursor VPg-Pro act to relieve translational repression, VPg supplemented
4
5 445 *in trans* stimulated viral RNA translation in infected plants in an eIF4E/iso4E-dependent manner
6
7 446 (Eskelin *et al.* 2011). The stimulation depended on the presence of the 5' UTR, but not the 3' UTR,
8
9 447 which is in agreement with the observation that the potyviral IRES-mediated translation is
10
11 448 refractory to repression via small RNA targets in the 3' UTR (Iwakawa and Tomari 2013).
12
13 449 Interestingly, VPg was unable to stimulate translation of a truncated viral RNA lacking all protein-
14
15 450 coding sequences except P1 (Eskelin, *et al.* 2011), suggesting a functional cooperation between
16
17 451 VPg and other viral proteins such as HCPro and CI. The possibility of such cooperation is also
18
19 452 supported by the fact that HCPro, similarly to VPg, interacts with eIF4E/iso4E and contains a 4E
20
21 453 binding motif (Ala-Poikela, *et al.* 2011). In addition to eIF4E/iso4E, another cellular protein, the
22
23 454 ribosomal stalk protein P0, is also required for the VPg-mediated stimulation of viral RNA
24
25 455 translation (Hafren *et al.* 2013). Exogenous expression of P0 alone was sufficient to increase viral
26
27 456 RNA translation and its co-expression with VPg exerted a further synergistic effect. As in the case
28
29 457 of VPg, the P0-mediated stimulation of viral RNA translation also depended on the presence of the
30
31 458 5' UTR, but not the 3' UTR (Hafren, *et al.* 2013), again suggesting a mechanism involving relief of
32
33 459 translational repression.

34
35
36
37
38 460 At a first glance, it is not easy to understand why CI would associate with ribosomes
39
40 461 together with HCPro and VPg-Pro. CI is a multifunctional protein involved in virus replication and
41
42 462 movement (Sorel *et al.* 2014), which contains twelve highly conserved sequence motifs that are
43
44 463 typically found in DExD/H-box helicases of the super family 2 (SF2) (Fairman-Williams *et al.*
45
46 464 2010). Cellular SF2 helicases take part in many important biological processes such as ribosome
47
48 465 biogenesis, translation, splicing, transcription, RNA decay and nuclear export (reviewed in
49
50 466 Jarmoskaite and Russell 2014). Mechanistically, the majority of cellular SF2 helicases act as RNA
51
52 467 chaperones, promoting RNA conformational rearrangements and remodeling of ribonucleoprotein
53
54 468 complexes (RNPs) (Jankowsky and Bowers 2006, Jarmoskaite and Russell 2014). Therefore, it is
55
56
57
58
59
60

possible that the potyviral SF2 helicase CI also functions as an RNP remodeling factor. In this case, the potyviral ribosome-associated complexes could rely on CI for assembly and function in the same way as large cellular RNPs rely on cellular SF2 helicases (Jarmoskaite and Russell 2014). Alternatively, the DExD/H-box helicase CI might directly relieve translational repression by displacing RISC from viral RNA (Fig. 8d) or by other mechanisms such as preventing the RISC-induced dissociation of eIF4A from IRES (Fig. 8c). It may even be possible that CI functionally replaces eIF4A, in a manner similar to how other cellular helicases replace eIF4A in quiescent cells (Bush *et al.* 2009), thereby making the initiation complex resistant to the RISC-mediated repression. In any case, it is conceivable that CI may act together with HCPro and VPg-Pro to relieve repression of viral RNA translation in infected cells, which is an intriguing possibility that warrants further investigation.

Taken together, the results of the present study suggest two putative mechanisms by which HCPro may exert its RNA silencing suppressor function. The first mechanism involves hijacking of the methionine cycle through the inhibition of SAMS and SAHH to block sRNA methylation by HEN1. The second mechanism is the relief of viral RNA translational repression through the interaction of the core RISC component AGO1 with the ribosome-associated, virus-specific complex composed of HCPro, CI and VPg/VPg-Pro. These mechanisms are not mutually exclusive, may overlap spatially and temporally and may both contribute to the suppression of antiviral RNA silencing. Future studies should examine these putative mechanisms in more detail. For example, it would be interesting to investigate the effect of HCPro on translational repression using catalytically inactive AGO1 mutants devoid of mRNA cleavage activity. There is no doubt that in the coming years we will continue to expand our knowledge and understanding of how viruses suppress RNA silencing, and of other defense and counter-defense mechanisms that have co-evolved in viruses and their hosts over millions of years of evolution.

EXPERIMENTAL PROCEDURES

Plants, viruses and expression constructs

Nicotiana benthamiana plants were grown in soil at 22°C, 50% relative humidity under 16h light/8h dark photoperiod in an environmentally controlled greenhouse. The transgenic *N. benthamiana* line 6j constitutively expressing FLAG-tagged *A. thaliana* RPL18B was a kind gift from Prof. Peter Moffett (Université de Sherbrooke, Canada).

The constructs generated in this study and described previously are listed in Supplementary Table S1. Viral constructs were based on the full-length infectious cDNA clone of PVA strain B11 (GenBank accession number AJ296311). The sequence of the twin Strep-tag II (2xStrep or Strep-tag III) has been described previously (Junttila *et al.* 2005). Plasmids were constructed using standard molecular cloning techniques and using Gateway technology (Life Technologies, Thermo Fisher Scientific, USA).

Strep-tag affinity purification of HCPro

HCPro-associated protein complexes were isolated from upper leaves systemically infected with the recombinant PVA expressing HCPro fused to the red fluorescent protein (RFP) and two copies of the Strep-tag II (HCPro^{(2xStrep)-RFP}). Leaves infected with PVA without the Strep-tag were used as a nonspecific binding control. Five grams of frozen, pulverized leaf tissue was mixed with 15 ml of pre-chilled PG buffer (100 mM Tris-HCl (pH 8.0), 150 mM NaCl, 5% (w/v) sucrose, 1 mM PMSF). The suspension was filtered through Miracloth and centrifuged at 3000xg for 5 min at 4°C to clear the lysate. The supernatant was transferred to a fresh tube and NP-40 was added to a final concentration of 0.1% (v/v). Avidin was also added to a final concentration of 100 µg/ml in order to minimize the binding of endogenous biotinylated proteins to the resin. The resulting samples were mixed with 500 µl of 50% Strep-Tactin MacroPrep resin suspension, pre-equilibrated with PG buffer, and placed on a rotator for 45 min at 4°C. The resulting resin-bound complexes were gently pelleted by centrifugation at 500xg for 5 min at 4°C and washed with 1 ml PG buffer. The re-suspended pellet was transferred to a microcentrifuge tube and centrifuged for 1 min at 500xg at 4°C. The wash was repeated three times in order to ensure the removal of unbound proteins. Bound protein complexes were eluted from the resin with 1 ml of 1 mM biotin in PG buffer, on a rotator, for 10 min at 4°C. Samples were centrifuged at 3000xg for 5 min at 4°C and the supernatant was carefully transferred to a fresh tube. A 200 µl aliquot of each purified sample was collected for LC-MS/MS analysis and the rest was stored at -80°C for subsequent analysis by SDS-PAGE and

Western blotting. The purification method described above was repeated three times, under the same conditions, using individually cultivated plant batches to account for natural plant-to-plant differences and variations in cultivation conditions.

SAMS activity measurements

SAMS activity was measured in *N. benthamiana* leaf extracts as described previously (Shen, *et al.* 2002) with modifications described in Supporting information.

Immunoaffinity purification of ribosomes for LC-MS/MS analysis

Ribosomes were isolated from *N. benthamiana* leaves using the previously published protocol for *A. thaliana* (Zanetti, *et al.* 2005) with modifications described in Supporting information.

Other methods

Other methods used in the present study are described in Supporting information.

ACKNOWLEDGEMENTS

We thank Minna Pöllänen for growing the plants for this study, Sini Miettinen for assistance with the LC-MS/MS analysis, Kaj-Roger Hurme for assistance with the isotope experiments, Prof. Peter Moffett for the generous gift of transgenic *N. benthamiana* lines constitutively expressing FLAG-tagged *A. thaliana* RPL18B, Prof. Raimo Tuominen for providing phosphocellulose paper and Dr. Jarkko Isotalo for assistance with statistical analysis. Ultracentrifugation was carried out at the Instruct Centre for Virus Production (ICVIR) at the University of Helsinki. No conflict of interest is declared. This work was supported by the Academy of Finland (grants 1138329 to K.M., 127969 to K.E. and 1258978 to M.V.). A.L. was supported by the Integrative Life Science Doctoral Program, M.B. by Jenny and Antti Wihuri Foundation and Department of Food and Environmental Sciences and S.D. by Erasmus Mundus Action 2 program BRAVE.

SUPPORTING INFORMATION

Additional Supporting Information may be found in the online version of this article.

1
2
3 557 **Figure S1.** Analysis of affinity-purified HCPro complexes by SDS-PAGE and silver staining.
4
5 558 **Figure S2.** The use of SAMS knockdown for background subtraction in SAMS activity assays.
6
7 559 **Figure S3.** HCPro, when expressed alone, is unable to inhibit the enzymatic activity of SAMS.
8
9 560 **Figure S4.** Light emitted by the Rluc- and Fluc-catalyzed bioluminescent reactions (in relative light
10 units; RLU), measured in the experiments shown in Fig. 4a.
11
12 561
13 562 **Figure S5.** SAMS and SAHH knock down can only partially rescue the loss of HCPro in PVA.
14
15 563 **Figure S6.** Overexposed image of the anti-GFP Western blot from Figure 6a.
16
17 564 **Figure S7.** Rabbit polyclonal antibody against the N-terminal peptide of *A. thaliana* AGO1
18 (AtAGO1) recognizes AGO1 from *N. Benthamiana* (NbAGO1).
19
20 565
21 566 **Figure S8.** Detection of HCPro and AGO1 in large ribosome-associated protein complexes from
22 virus-infected plants.
23
24 567
25 568 **Table S1.** Recombinant constructs used in this study.
26
27 569
28
29
30
31
32
33 570 REFERENCES
34
35

36 571 **Ala-Poikela, M., Goytia, E., Haikonen, T., Rajamaki, M.L. and Valkonen, J.P.** (2011) Helper component
37 572 proteinase of the genus Potyvirus is an interaction partner of translation initiation factors eIF(iso)4E
38 573 and eIF4E and contains a 4E binding motif. *Journal of virology*, **85**, 6784-6794.
39 574 **Anandalakshmi, R., Marathe, R., Ge, X., Herr, J.M., Jr., Mau, C., Mallory, A., Pruss, G., Bowman, L. and**
40 575 **Vance, V.B.** (2000) A calmodulin-related protein that suppresses posttranscriptional gene silencing
41 576 in plants. *Science*, **290**, 142-144.
42 577 **Anandalakshmi, R., Pruss, G.J., Ge, X., Marathe, R., Mallory, A.C., Smith, T.H. and Vance, V.B.** (1998) A
43 578 viral suppressor of gene silencing in plants. *Proc Natl Acad Sci U S A*, **95**, 13079-13084.
44 579 **Ballut, L., Drucker, M., Pugniere, M., Cambon, F., Blanc, S., Roquet, F., Candresse, T., Schmid, H.P.,**
45 580 **Nicolas, P., Gall, O.L. and Badaoui, S.** (2005) HcPro, a multifunctional protein encoded by a plant
46 581 RNA virus, targets the 20S proteasome and affects its enzymic activities. *The Journal of general*
47 582 *virology*, **86**, 2595-2603.
48 583 **Barakat, A., Szick-Miranda, K., Chang, I.F., Guyot, R., Blanc, G., Cooke, R., Delseny, M. and Bailey-Serres, J.**
49 584 (2001) The organization of cytoplasmic ribosomal protein genes in the Arabidopsis genome. *Plant*
50 585 *physiology*, **127**, 398-415.
51 586 **Bologna, N.G. and Voinnet, O.** (2014) The diversity, biogenesis, and activities of endogenous silencing small
52 587 RNAs in Arabidopsis. *Annual review of plant biology*, **65**, 473-503.
53 588 **Brigneti, G., Voinnet, O., Li, W.X., Ji, L.H., Ding, S.W. and Baulcombe, D.C.** (1998) Viral pathogenicity
54 589 determinants are suppressors of transgene silencing in Nicotiana benthamiana. *EMBO J*, **17**, 6739-
55 590 6746.
56
57
58
59
60

- Brodersen, P., Sakvarelidze-Achard, L., Bruun-Rasmussen, M., Dunoyer, P., Yamamoto, Y.Y., Sieburth, L. and Voinnet, O. (2008) Widespread translational inhibition by plant miRNAs and siRNAs. *Science*, **320**, 1185-1190.
- Bush, M.S., Hutchins, A.P., Jones, A.M., Naldrett, M.J., Jarmolowski, A., Lloyd, C.W. and Doonan, J.H. (2009) Selective recruitment of proteins to 5' cap complexes during the growth cycle in Arabidopsis. *The Plant journal : for cell and molecular biology*, **59**, 400-412.
- Canizares, M.C., Lozano-Duran, R., Canto, T., Bejarano, E.R., Bisaro, D.M., Navas-Castillo, J. and Moriones, E. (2013) Effects of the crinivirus coat protein-interacting plant protein SAHH on post-transcriptional RNA silencing and its suppression. *Molecular plant-microbe interactions : MPMI*, **26**, 1004-1015.
- Carrington, J.C. and Herndon, K.L. (1992) Characterization of the potyviral HC-pro autoproteolytic cleavage site. *Virology*, **187**, 308-315.
- Chang, I.F., Szick-Miranda, K., Pan, S. and Bailey-Serres, J. (2005) Proteomic characterization of evolutionarily conserved and variable proteins of Arabidopsis cytosolic ribosomes. *Plant physiology*, **137**, 848-862.
- Chiu, M.H., Chen, I.H., Baulcombe, D.C. and Tsai, C.H. (2010) The silencing suppressor P25 of Potato virus X interacts with Argonaute1 and mediates its degradation through the proteasome pathway. *Molecular plant pathology*, **11**, 641-649.
- Chung, B.Y., Miller, W.A., Atkins, J.F. and Firth, A.E. (2008) An overlapping essential gene in the Potyviridae. *Proc Natl Acad Sci U S A*, **105**, 5897-5902.
- Clarke, S. and Banfield, K. (2001) S-adenosylmethionine-dependent methyltransferases. In *Homocysteine in Health and Disease* (Carmel, R. and Jacobsen, D.W. eds). Cambridge, U.K.: Cambridge University Press, pp. 63-78.
- Ebhardt, H.A., Thi, E.P., Wang, M.B. and Unrau, P.J. (2005) Extensive 3' modification of plant small RNAs is modulated by helper component-proteinase expression. *Proc Natl Acad Sci U S A*, **102**, 13398-13403.
- Endres, M.W., Gregory, B.D., Gao, Z., Foreman, A.W., Mlotshwa, S., Ge, X., Pruss, G.J., Ecker, J.R., Bowman, L.H. and Vance, V. (2010) Two plant viral suppressors of silencing require the ethylene-inducible host transcription factor RAV2 to block RNA silencing. *PLoS pathogens*, **6**, e1000729.
- Eskelin, K., Hafren, A., Rantalainen, K.I. and Makinen, K. (2011) Potyviral VPg enhances viral RNA Translation and inhibits reporter mRNA translation in planta. *Journal of virology*, **85**, 9210-9221.
- Fabian, M.R., Sonenberg, N. and Filipowicz, W. (2010) Regulation of mRNA translation and stability by microRNAs. *Annual review of biochemistry*, **79**, 351-379.
- Fairman-Williams, M.E., Guenther, U.P. and Jankowsky, E. (2010) SF1 and SF2 helicases: family matters. *Current opinion in structural biology*, **20**, 313-324.
- Fukao, A., Mishima, Y., Takizawa, N., Oka, S., Imataka, H., Pelletier, J., Sonenberg, N., Thoma, C. and Fujiwara, T. (2014) MicroRNAs trigger dissociation of eIF4A1 and eIF4AII from target mRNAs in humans. *Mol Cell*, **56**, 79-89.
- Fukaya, T., Iwakawa, H.O. and Tomari, Y. (2014) MicroRNAs block assembly of eIF4F translation initiation complex in Drosophila. *Mol Cell*, **56**, 67-78.
- Gallie, D.R. (2001) Cap-independent translation conferred by the 5' leader of tobacco etch virus is eukaryotic initiation factor 4G dependent. *Journal of virology*, **75**, 12141-12152.
- Garcia-Ruiz, H., Carbonell, A., Hoyer, J.S., Fahlgren, N., Gilbert, K.B., Takeda, A., Giampetruzzi, A., Garcia Ruiz, M.T., McGinn, M.G., Lowery, N., Martinez Baladejo, M.T. and Carrington, J.C. (2015) Roles and programming of Arabidopsis ARGONAUTE proteins during Turnip mosaic virus infection. *PLoS pathogens*, **11**, e1004755.
- Govier, D.A., Kassanis, B. and Pirone, T.P. (1977) Partial purification and characterization of the potato virus Y helper component. *Virology*, **78**, 306-314.
- Guo, D., Rajamaki, M.L., Saarma, M. and Valkonen, J.P. (2001) Towards a protein interaction map of potyviruses: protein interaction matrixes of two potyviruses based on the yeast two-hybrid system. *The Journal of general virology*, **82**, 935-939.

1
2
3 642 **Guo, D., Spetz, C., Saarma, M. and Valkonen, J.P.** (2003) Two potato proteins, including a novel RING finger
4 643 protein (HIP1), interact with the potyviral multifunctional protein HCpro. *Molecular plant-microbe*
5 644 *interactions : MPMI*, **16**, 405-410.
6 645 **Hafren, A., Eskelin, K. and Makinen, K.** (2013) Ribosomal protein P0 promotes Potato virus A infection and
7 646 functions in viral translation together with VPg and eIF(iso)4E. *Journal of virology*, **87**, 4302-4312.
8 647 **Haikonen, T., Rajamaki, M.L. and Valkonen, J.P.** (2013) Interaction of the microtubule-associated host
9 648 protein HIP2 with viral helper component proteinase is important in infection with potato virus A.
10 649 *Molecular plant-microbe interactions : MPMI*, **26**, 734-744.
11 650 **Horwich, M.D., Li, C., Matranga, C., Vagin, V., Farley, G., Wang, P. and Zamore, P.D.** (2007) The Drosophila
12 651 RNA methyltransferase, DmHen1, modifies germline piRNAs and single-stranded siRNAs in RISC.
13 652 *Current biology : CB*, **17**, 1265-1272.
14 653 **Hummel, M., Cordewener, J.H., de Groot, J.C., Smeekens, S., America, A.H. and Hanson, J.** (2012) Dynamic
15 654 protein composition of Arabidopsis thaliana cytosolic ribosomes in response to sucrose feeding as
16 655 revealed by label free MSE proteomics. *Proteomics*, **12**, 1024-1038.
17 656 **Hutvagner, G. and Zamore, P.D.** (2002) A microRNA in a multiple-turnover RNAi enzyme complex. *Science*,
18 657 **297**, 2056-2060.
19 658 **Iwakawa, H.O. and Tomari, Y.** (2013) Molecular insights into microRNA-mediated translational repression
20 659 in plants. *Mol Cell*, **52**, 591-601.
21 660 **Jamous, R.M., Boonrod, K., Fuellgrabe, M.W., Ali-Shtayeh, M.S., Krczal, G. and Wassenegger, M.** (2011)
22 661 The helper component-proteinase of the Zucchini yellow mosaic virus inhibits the Hua Enhancer 1
23 662 methyltransferase activity in vitro. *The Journal of general virology*, **92**, 2222-2226.
24 663 **Jankowsky, E. and Bowers, H.** (2006) Remodeling of ribonucleoprotein complexes with DEXH/D RNA
25 664 helicases. *Nucleic acids research*, **34**, 4181-4188.
26 665 **Jarmoskaite, I. and Russell, R.** (2014) RNA helicase proteins as chaperones and remodelers. *Annual review*
27 666 *of biochemistry*, **83**, 697-725.
28 667 **Jones-Rhoades, M.W., Bartel, D.P. and Bartel, B.** (2006) MicroRNAs and their regulatory roles in plants.
29 668 *Annual review of plant biology*, **57**, 19-53.
30 669 **Junttila, M.R., Saarinen, S., Schmidt, T., Kast, J. and Westermarck, J.** (2005) Single-step Strep-tag
31 670 purification for the isolation and identification of protein complexes from mammalian cells.
32 671 *Proteomics*, **5**, 1199-1203.
33 672 **Kasschau, K.D. and Carrington, J.C.** (1995) Requirement for HC-Pro processing during genome amplification
34 673 of tobacco etch potyvirus. *Virology*, **209**, 268-273.
35 674 **Kasschau, K.D. and Carrington, J.C.** (1998) A counterdefensive strategy of plant viruses: suppression of
36 675 posttranscriptional gene silencing. *Cell*, **95**, 461-470.
37 676 **Lakatos, L., Csorba, T., Pantaleo, V., Chapman, E.J., Carrington, J.C., Liu, Y.P., Dolja, V.V., Calvino, L.F.,**
38 677 **Lopez-Moya, J.J. and Burgyan, J.** (2006) Small RNA binding is a common strategy to suppress RNA
39 678 silencing by several viral suppressors. *EMBO J*, **25**, 2768-2780.
40 679 **Lanet, E., Delannoy, E., Sormani, R., Floris, M., Brodersen, P., Crete, P., Voinnet, O. and Robaglia, C.**
41 680 (2009) Biochemical evidence for translational repression by Arabidopsis microRNAs. *The Plant cell*,
42 681 **21**, 1762-1768.
43 682 **Lee, S., Doxey, A.C., McConkey, B.J. and Moffatt, B.A.** (2012) Nuclear targeting of methyl-recycling
44 683 enzymes in Arabidopsis thaliana is mediated by specific protein interactions. *Molecular plant*, **5**,
45 684 231-248.
46 685 **Li, J., Yang, Z., Yu, B., Liu, J. and Chen, X.** (2005) Methylation protects miRNAs and siRNAs from a 3'-end
47 686 uridylation activity in Arabidopsis. *Current biology : CB*, **15**, 1501-1507.
48 687 **Li, S., Liu, L., Zhuang, X., Yu, Y., Liu, X., Cui, X., Ji, L., Pan, Z., Cao, X., Mo, B., Zhang, F., Raikhel, N., Jiang, L.**
49 688 **and Chen, X.** (2013) MicroRNAs inhibit the translation of target mRNAs on the endoplasmic
50 689 reticulum in Arabidopsis. *Cell*, **153**, 562-574.
51 690 **Lozsa, R., Csorba, T., Lakatos, L. and Burgyan, J.** (2008) Inhibition of 3' modification of small RNAs in virus-
52 691 infected plants require spatial and temporal co-expression of small RNAs and viral silencing-
53 692 suppressor proteins. *Nucleic acids research*, **36**, 4099-4107.

- Mallory, A.C., Ely, L., Smith, T.H., Marathe, R., Anandalakshmi, R., Fagard, M., Vaucheret, H., Pruss, G., Bowman, L. and Vance, V.B.** (2001) HC-Pro suppression of transgene silencing eliminates the small RNAs but not transgene methylation or the mobile signal. *The Plant cell*, **13**, 571-583.
- Martinez, F. and Daros, J.A.** (2014) Tobacco etch virus protein P1 traffics to the nucleolus and associates with the host 60S ribosomal subunits during infection. *Journal of virology*, **88**, 10725-10737.
- Mustroph, A., Zanetti, M.E., Jang, C.J., Holtan, H.E., Repetti, P.P., Galbraith, D.W., Girke, T. and Bailey-Serres, J.** (2009) Profiling translomes of discrete cell populations resolves altered cellular priorities during hypoxia in Arabidopsis. *Proc Natl Acad Sci U S A*, **106**, 18843-18848.
- Pirone, T.P. and Blanc, S.** (1996) Helper-dependent vector transmission of plant viruses. *Annual review of phytopathology*, **34**, 227-247.
- Pitkanen, L., Tuomainen, P. and Eskelin, K.** (2014) Analysis of plant ribosomes with asymmetric flow field-flow fractionation. *Analytical and bioanalytical chemistry*, **406**, 1629-1637.
- Pruss, G., Ge, X., Shi, X.M., Carrington, J.C. and Bowman Vance, V.** (1997) Plant viral synergism: the potyviral genome encodes a broad-range pathogenicity enhancer that transactivates replication of heterologous viruses. *The Plant cell*, **9**, 859-868.
- Pumplin, N. and Voinnet, O.** (2013) RNA silencing suppression by plant pathogens: defence, counter-defence and counter-counter-defence. *Nature reviews. Microbiology*, **11**, 745-760.
- Rajamaki, M.L. and Valkonen, J.P.** (2009) Control of nuclear and nucleolar localization of nuclear inclusion protein a of picorna-like Potato virus A in Nicotiana species. *The Plant cell*, **21**, 2485-2502.
- Ramachandran, V. and Chen, X.** (2008) Degradation of microRNAs by a family of exoribonucleases in Arabidopsis. *Science*, **321**, 1490-1492.
- Redondo, E., Krause-Sakate, R., Yang, S.J., Lot, H., Le Gall, O. and Candresse, T.** (2001) Lettuce mosaic virus pathogenicity determinants in susceptible and tolerant lettuce cultivars map to different regions of the viral genome. *Molecular plant-microbe interactions : MPMI*, **14**, 804-810.
- Reynoso, M.A., Blanco, F.A., Bailey-Serres, J., Crespi, M. and Zanetti, M.E.** (2012) Selective recruitment of mRNAs and miRNAs to polyribosomes in response to rhizobia infection in Medicago truncatula. *The Plant journal : for cell and molecular biology*.
- Reytor, E., Perez-Miguelsanz, J., Alvarez, L., Perez-Sala, D. and Pajares, M.A.** (2009) Conformational signals in the C-terminal domain of methionine adenosyltransferase I/III determine its nucleocytoplasmic distribution. *FASEB journal : official publication of the Federation of American Societies for Experimental Biology*, **23**, 3347-3360.
- Robaglia, C. and Caranta, C.** (2006) Translation initiation factors: a weak link in plant RNA virus infection. *Trends in plant science*, **11**, 40-45.
- Rojas, M.R., Zerbini, F.M., Allison, R.F., Gilbertson, R.L. and Lucas, W.J.** (1997) Capsid protein and helper component-proteinase function as potyvirus cell-to-cell movement proteins. *Virology*, **237**, 283-295.
- Roossinck, M.J.** (2012) Plant virus metagenomics: biodiversity and ecology. *Annu Rev Genet*, **46**, 359-369.
- Roudet-Tavert, G., Michon, T., Walter, J., Delaunay, T., Redondo, E. and Le Gall, O.** (2007) Central domain of a potyvirus VPg is involved in the interaction with the host translation initiation factor eIF4E and the viral protein HcPro. *The Journal of general virology*, **88**, 1029-1033.
- Saenz, P., Salvador, B., Simon-Mateo, C., Kasschau, K.D., Carrington, J.C. and Garcia, J.A.** (2002) Host-specific involvement of the HC protein in the long-distance movement of potyviruses. *Journal of virology*, **76**, 1922-1931.
- Sahana, N., Kaur, H., Basavaraj, Tena, F., Jain, R.K., Palukaitis, P., Canto, T. and Praveen, S.** (2012) Inhibition of the host proteasome facilitates papaya ringspot virus accumulation and proteasomal catalytic activity is modulated by viral factor HcPro. *PLoS One*, **7**, e52546.
- Schmidt, T.G. and Skerra, A.** (2007) The Strep-tag system for one-step purification and high-affinity detection or capturing of proteins. *Nature protocols*, **2**, 1528-1535.
- Scholthof, K.B., Adkins, S., Czosnek, H., Palukaitis, P., Jacquot, E., Hohn, T., Hohn, B., Saunders, K., Candresse, T., Ahlquist, P., Hemenway, C. and Foster, G.D.** (2011) Top 10 plant viruses in molecular plant pathology. *Molecular plant pathology*, **12**, 938-954.

Shen, B., Li, C. and Tarczynski, M.C. (2002) High free-methionine and decreased lignin content result from a mutation in the Arabidopsis S-adenosyl-L-methionine synthetase 3 gene. *The Plant journal : for cell and molecular biology*, **29**, 371-380.

Shi, X.M., Miller, H., Verchot, J., Carrington, J.C. and Vance, V.B. (1997) Mutations in the region encoding the central domain of helper component-proteinase (HC-Pro) eliminate potato virus X/potyviral synergism. *Virology*, **231**, 35-42.

Shiboleth, Y.M., Haronsky, E., Leibman, D., Arazi, T., Wassenegger, M., Whitham, S.A., Gaba, V. and Gal-On, A. (2007) The conserved FRNK box in HC-Pro, a plant viral suppressor of gene silencing, is required for small RNA binding and mediates symptom development. *Journal of virology*, **81**, 13135-13148.

Sorel, M., Garcia, J.A. and German-Retana, S. (2014) The Potyviridae cylindrical inclusion helicase: a key multipartner and multifunctional protein. *Molecular plant-microbe interactions : MPMI*, **27**, 215-226.

Truniger, V. and Aranda, M.A. (2009) Recessive resistance to plant viruses. *Advances in virus research*, **75**, 119-159.

Valli, A., Gallo, A., Calvo, M., de Jesus Perez, J. and Garcia, J.A. (2014) A novel role of the potyviral helper component proteinase contributes to enhance the yield of viral particles. *Journal of virology*, **88**, 9808-9818.

Verchot, J., Herndon, K.L. and Carrington, J.C. (1992) Mutational analysis of the tobacco etch potyviral 35-kDa proteinase: identification of essential residues and requirements for autoproteolysis. *Virology*, **190**, 298-306.

Voss, S. and Skerra, A. (1997) Mutagenesis of a flexible loop in streptavidin leads to higher affinity for the Strep-tag II peptide and improved performance in recombinant protein purification. *Protein engineering*, **10**, 975-982.

Wang, A. and Krishnaswamy, S. (2012) Eukaryotic translation initiation factor 4E-mediated recessive resistance to plant viruses and its utility in crop improvement. *Molecular plant pathology*, **13**, 795-803.

Wang, Y., Gaba, V., Yang, J., Palukaitis, P. and Gal-On, A. (2002) Characterization of Synergy Between Cucumber mosaic virus and Potyviruses in Cucurbit Hosts. *Phytopathology*, **92**, 51-58.

Wei, T., Huang, T.S., McNeil, J., Laliberte, J.F., Hong, J., Nelson, R.S. and Wang, A. (2010) Sequential recruitment of the endoplasmic reticulum and chloroplasts for plant potyvirus replication. *Journal of virology*, **84**, 799-809.

Yambao, M.L., Masuta, C., Nakahara, K. and Uyeda, I. (2003) The central and C-terminal domains of VPg of Clover yellow vein virus are important for VPg-HCPro and VPg-VPg interactions. *The Journal of general virology*, **84**, 2861-2869.

Yang, Z., Ebright, Y.W., Yu, B. and Chen, X. (2006) HEN1 recognizes 21-24 nt small RNA duplexes and deposits a methyl group onto the 2' OH of the 3' terminal nucleotide. *Nucleic acids research*, **34**, 667-675.

Yu, B., Chapman, E.J., Yang, Z., Carrington, J.C. and Chen, X. (2006) Transgenically expressed viral RNA silencing suppressors interfere with microRNA methylation in Arabidopsis. *FEBS letters*, **580**, 3117-3120.

Yu, B., Yang, Z., Li, J., Minakhina, S., Yang, M., Padgett, R.W., Steward, R. and Chen, X. (2005) Methylation as a crucial step in plant microRNA biogenesis. *Science*, **307**, 932-935.

Zanetti, M.E., Chang, I.F., Gong, F., Galbraith, D.W. and Bailey-Serres, J. (2005) Immunopurification of polyribosomal complexes of Arabidopsis for global analysis of gene expression. *Plant physiology*, **138**, 624-635.

Zilian, E. and Maiss, E. (2011) Detection of plum pox potyviral protein-protein interactions in planta using an optimized mRFP-based bimolecular fluorescence complementation system. *The Journal of general virology*, **92**, 2711-2723.

794 Table 1. Viral and host proteins associated with HCPro in total extracts of PVA-infected cells

<i>Protein</i>	<i>Av. PSM^a</i> <i>control</i> <i>purification</i>	<i>SD</i>	<i>Av. PSM</i> <i>HCpro^{2xStrep-RFP}</i> <i>purification</i>	<i>SD</i>	<i>Western</i> <i>blot</i> <i>validation</i> <i>n</i>	<i>Independent</i> <i>validation</i>
HCPro^{2xStrepRFP} (bait protein)	23	27	605	64	+	Plisson et al., 2003 (HCPro dimerisation)
CI	0.3	0.6	7.3	4.2	+	Guo et al., 2001
VPg-Pro	0	0	0.67	0.58	+	Roudet-Tavert et al., 2007
SAMS1	0	0	1	0	+	-
SAHH1	0	0	0.67	1.2	nv ^b	Canizares et al., 2013

795 a. Average PSM value calculated with three biological replicates.

796 b. Not validated by Western blotting

798 Table 2. PVA proteins associated with ribosomes

<i>Protein</i>	<i>Av. PSM^a</i> <i>non-tg + PVA inf.</i>	<i>Av. PSM</i> <i>tg + PVA inf.</i>	<i>Western</i> <i>blot validation</i>
FLAG-RPL18b (bait protein)	0.3	8	+
CI	0	10.8	+
HCpro	0	12	+
VPg/VPg-Pro	0	1.25	nd ^b

799 a. Average PSM value calculated with two biological and two technical replicates at 4 dpi

800 b. Not detected by Western blotting

1
2
3
4
5
6
7
8
9
10
11
12
13
14
15
16
17
18
19
20
21
22
23
24
25
26
27
28
29
30
31
32
33
34
35
36
37
38
39
40
41
42
43
44
45
46
47
48
49
50
51
52
53
54
55
56
57
58
59
60

FIGURE LEGENDS

Figure 1. HCPro forms stable complexes in systemically infected plants with enzymes involved in the methionine cycle, ribosomal proteins and viral proteins VPg-Pro and CI. A) Schematic representation of the HCPro purification procedure. The workflow includes systemic infection of *N. benthamiana* plants with recombinant PVA expressing HCPro fused to two copies of the Strep tag (2xStrep) and RFP, binding of the fusion protein and its associated proteins to the Strep-Tactin resin, washing away of unbound proteins, elution of the protein complexes with biotin and their analysis by LC-MS/MS. Selected HCPro binding partners identified by LC-MS/MS are listed in the table below. B) Validation of the HCPro^{(2xStrep)-RFP} purification procedure by Western blotting. Three independent biological replicates of HCPro^{(2xStrep)-RFP} purification were analyzed in parallel with three purification controls from plants infected with the wild type virus having no affinity tags in the polyprotein sequence. The control lane (ctrl) represents a total lysate of cells infected with PVA-HCPro^{(2xStrep)-RFP}. C) Validation of the selected HCPro binding partners by Western blotting. Purified HCPro complexes were analyzed as in (B) with antibodies against VPg, CI and S-adenosyl-L-methionine synthase 1 (SAMS1). Arrowheads indicate the positions of monomeric proteins. Western blots were deliberately overexposed to confirm the absence of signal in the controls. The positions of molecular mass markers are shown in kDa on the left of each panel.

Figure 2. Large multiprotein complexes formed by HCPro in systemically infected plants simultaneously contain SAMS, CI, AGO1 and VPg (VPg-Pro). Protein sample purified as described in Fig. 1 was separated by SDS-PAGE on a single wide lane and transferred to a blotting membrane. The membrane was cut into equal strips and probed with antibodies against HC-Pro, SAMS1, CI, AGO1 or VPg. Note that all antibodies recognized a band of the same electrophoretic mobility. The positions of molecular mass markers are shown in kDa on the left.

826

Figure 3. PVA infection inhibits SAMS enzymatic activity whereas PVA Δ HCPPro expression

doesn't. A) *N. benthamiana* leaves were infiltrated with *A. tumefaciens* strains carrying cDNA of PVA (PVA), cDNA of PVA lacking the HCPPro sequence (PVA Δ HCPPro) or a control vector expressing an irrelevant β -glucuronidase gene (GUS). At 5 days post-infiltration, total SAMS enzymatic activity was assayed in leaf extracts by measuring the radioactivity incorporated into SAM from ^{35}S -labeled L-methionine (Met) in the presence of ATP. Prior to radioactivity measurements, ^{35}S -labeled SAM was separated from ^{35}S -Met using phosphocellulose cation exchange paper. Background subtraction was carried out as described in Fig. S2. Two independent experiments were carried out with two or three biological replicates, each of which was technically replicated three times. Data from one representative experiment is shown as a bar graph. The bars represent means of three biological replicates \pm standard error of the mean (SEM). A linear mixed-effects model, in which replication is treated as a random effect, was applied to examine whether SAMS enzymatic activity was affected by PVA infection. The table shows the results of statistical analysis using the mixed-effects model. The following significance codes are used: *** (<0.001), ** (<0.01), * (<0.05). B) The inhibition of SAMS activity in PVA-infected plants is not due to SAMS degradation. Upper panel: comparison of SAMS protein levels in mock- and PVA-infected cells by Western blotting. Lower panel: loading control showing Ponceau S-stained RuBisCO band on the blotting membrane.

845

Figure 4. Partial rescue of the HCPPro-deficient PVA phenotype by SAMS, SAHH and HEN1

knockdown. *N. benthamiana* leaves were co-infiltrated with *Agrobacterium* strains carrying cDNA of PVA lacking HCPPro (PVA Δ HCPPro) and expressing *Renilla* luciferase, a control reporter vector constitutively expressing Firefly luciferase and a silencing vector expressing hairpin RNAs

1
2
3 850 targeting *SAMS*, *SAHH* or *HENI*. In the negative control (CTRL), leaves were infiltrated with the
4
5 851 same *Agrobacterium* strains, except that the silencing vector lacked any RNA hairpin sequence.
6
7 852 *SAMS*, *SAHH* and *HENI* knockdown was confirmed by RT-PCR. A) Rluc activity was measured at
8
9 853 5 days post-inoculation and normalized to the Fluc activity. Note the increase in the normalized
10
11 854 viral gene expression induced by the knockdown of *SAMS* or *SAHH* and the synergistic effect
12
13 855 exhibited by the knockdown of both genes. The absolute luminescence values are presented in
14
15 856 supplementary Fig. S4. B) PVA Δ HCPro RNA copy numbers were quantified in the samples by
16
17 857 RT-PCR and normalized to expression of a housekeeping gene (PP2A). Note the accumulation of
18
19 858 viral RNA upon *SAMS* or *SAHH* knockdown. C) Rluc activity was measured at 5 days post-
20
21 859 inoculation and normalized to the Fluc activity. Note the accumulation of Rluc upon *HENI*
22
23 860 knockdown. Data are represented as means of five (A) or six (B) and (C) biological replicates \pm
24
25 861 standard error of the mean (SEM). Different letters above bars in (A) and (B) indicate significant
26
27 862 differences (t-test, $p < 0.05$). The same letter indicates no significant difference (t-test, $p > 0.1$). ***
28
29 863 denotes statistical significance ($p < 0.001$) in (C).
30
31
32
33
34
35 864

36
37
38 865 **Figure 5. HCPro, CI and VPg are bound to ribosomes in PVA-infected cells. A) Schematic**
39
40 866 **representation of the ribosome purification procedure.** Transgenic *N. benthamiana* plants
41
42 867 constitutively expressing the FLAG-tagged large subunit ribosomal protein L18B from *A. thaliana*
43
44 868 were infected with PVA through agroinfiltration. Ribosomes were purified from cytoplasmic
45
46 869 extracts of infected leaves using anti-FLAG immunoaffinity resin at 4 days post-infiltration.
47
48 870 Purified ribosomes were analyzed by LC-MS/MS for the presence of associated viral proteins.
49
50 871 Samples from PVA-infected non-transgenic plants were used as purification controls. B) Validation
51
52 872 of the ribosome purification procedure by SDS-PAGE/silver-staining (left panel) and Western
53
54 873 blotting with anti-FLAG antibody (right panel). Note the detection of characteristic low molecular
55
56 874 weight proteins in samples purified from transgenic (tg) plants, but not in purifications from non-
57
58
59
60

transgenic (non-tg) controls. The positions of molecular mass markers are shown in kDa. C) Validation of the ribosome quality and integrity by means of electrophoretic analysis of ribosomal RNA (rRNA). Note the similar rRNA integrity and ratio between 26S and 18S rRNA in the purified ribosomes and the total RNA sample. The positions of molecular mass markers are shown on the left in kilobases.

880

Figure 6. RNA silencing suppressor HCPro and AGO1, the core component of RISC, interact with each other and are both associated with ribosomes. A) AGO1 and HCPro form stable complexes *in planta*. The panel shows Western blot analysis of total lysates from cells co-expressing AGO1^{CFP} and HCPro. *N.benthamiana* leaves were infiltrated with *A.tumefaciens* carrying AGO1^{CFP} and HCPro or AGO1^{CFP} and a full-length infectious cDNA clone of PVA. In the negative controls, AGO1^{CFP} was co-expressed with an unrelated bacterial protein β -glucuronidase (GUS) or PVA lacking HCPro (PVA Δ HCPro). Note the formation of AGO1^{CFP} complexes in the presence of HCPro, but not in the controls. B) Endogenous AGO1 binds to HCPro in systemically infected *N. benthamiana* plants. Strep-tag-purified HCPro complexes (see Figure 1) were analyzed by Western blotting with anti-AGO1 antibody. Note the pull-down of AGO1 complexes with HCPro^{(2xStrep)-RFP} in all purification replicates, but not in the controls. C) HCPro and AGO1 are both associated with ribosomes. Transgenic plants constitutively expressing FLAG-tagged ribosomal protein L18B were infiltrated with *A.tumefaciens* carrying AGO1^{CFP} and HCPro^{RFP} or AGO1^{CFP} and PVA-HCPro^{(2xStrep)-RFP}. Ribosomes were purified in a two-step procedure involving ultracentrifugation in a continuous sucrose gradient followed by affinity purification on anti-FLAG resin. Purified ribosomes were analyzed by Western blotting for the presence of associated HCPro^{RFP} and AGO1^{CFP}. A sample from non-transgenic *N. benthamiana* was used as a negative control (left lane). Arrowheads indicate the positions of monomeric proteins and asterisks indicate

1
2
3 899 the positions of putative HCPro-AGO1 complexes. The positions of molecular mass markers are
4
5 900 shown in kDa on the left of each panel.
6
7
8 901

10
11 902 **Figure 7. Hypothetical model for the suppression of antiviral RNA silencing through local**
12
13 903 **disruption of the methionine cycle.** A) Schematic representation of the methionine cycle in non-
14
15 904 infected cells. SAMS catalyzes the conversion of methionine to SAM, which serves as a methyl
16
17 905 donor for HEN1. HEN1 methylates sRNAs, protecting them from degradation before their loading
18
19 906 onto RISC. The methylation reaction byproduct SAH is subsequently broken down by SAHH to
20
21 907 homocysteine, which is recycled back to methionine by MS. B) In potyvirus-infected cells, HCPro
22
23 908 acts together with other viral proteins to locally inhibit SAMS and SAHH. As a result, HEN1 is
24
25 909 deprived of its substrate SAM and poisoned by its feedback inhibitor SAH. This, in turn, leads to
26
27 910 the inhibition of sRNA methylation and suppression of RNA silencing via sRNA polyuridylation
28
29 911 and degradation. Circles represent enzymes and grey rectangles represent small molecules. Falling
30
31 912 levels of SAM and rising levels of SAH are indicated by arrows. SAM: S-adenosyl-L-methionine;
32
33 913 SAMS: S-adenosyl-L-methionine synthase; HEN1: HUA ENHANCER 1; SAH: S-adenosyl-L-
34
35 914 homocysteine; SAHH: S-adenosyl-L-homocysteine hydrolase; MS: methionine synthase.
36
37
38
39
40
41 915

42
43
44 916 **Figure 8. Hypothetical model for the relief of antiviral translational repression in potyvirus-**
45
46 917 **infected cells.** A-B) Putative plant-specific mechanisms of RISC-mediated translational repression.
47
48 918 sRNAs that are highly complementary to their targets in the 5' UTR or ORF are incorporated into
49
50 919 AGO1-RISC to repress mRNA translation either by inhibiting the initiation (A) or by sterically
51
52 920 hindering ribosome movement (B) (Iwakawa and Tomari, 2013). The mechanism responsible for
53
54 921 the inhibition of translation initiation may involve the AGO1-RISC-induced dissociation of the
55
56 922 DExD/H-box helicase eIF4A from target mRNA and/or steric hindrance of 40S ribosomal subunit
57
58
59
60

binding to the mRNA. C-D) In potyvirus-infected cells, HCPro may act together with CI and VPg/VPg-Pro to relieve translational repression of viral RNA. During the IRES-mediated initiation (C), virus-specific protein complexes could be formed with eIF4A, preventing the AGO1-RISC-induced dissociation of eIF4A (Fukao *et al.* 2014, Fukaya *et al.* 2014) from viral RNA. This allows the recruitment of preinitiation complexes to the IRES-bound eIF4F complex and subsequent initiation of translation. During this process, the viral DExD/H-box helicase CI might act as an RNP remodeling factor functionally assisting the initiation of translation. Although the direct involvement of the cap-binding protein eIF4E in the cap-independent initiation of potyviral RNA translation remains uncertain, the interaction of eIF4E with HCPro and VPg could assist the relief of viral RNA translational repression. Free VPg or its precursor VPg-Pro could be targeted to the eIF4F complex through interaction with eIF4E and/or dimerization with the VPg covalently attached to the 5' end of viral RNA. During translation elongation (D), viral proteins associated with ribosomes may induce the displacement of AGO1-RISC from viral RNA. The putative RNP remodeling activity of CI might play a role in this process, assisting the intrinsic ability of the ribosome to displace RNA-bound proteins in its path.

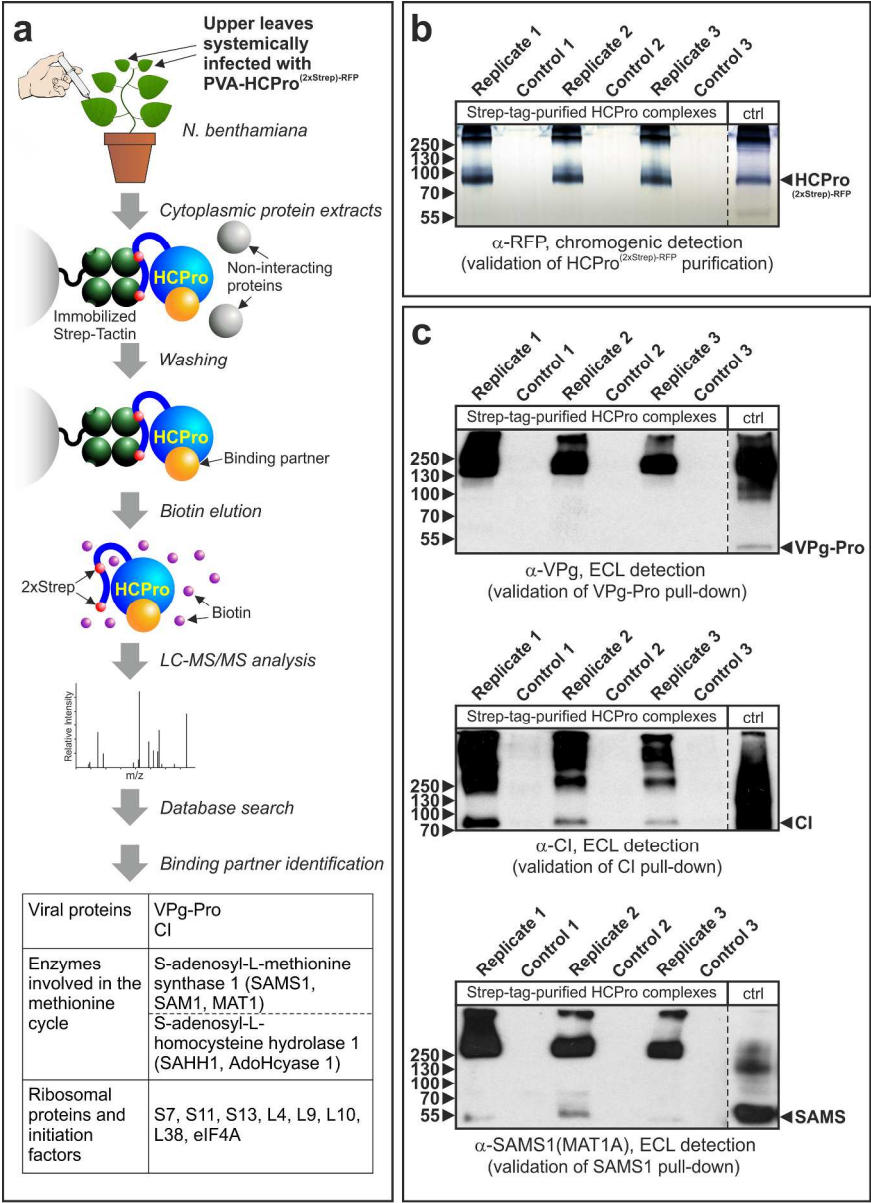


Figure 1. HCPro forms stable complexes in systemically infected plants with enzymes involved in the methionine cycle, ribosomal proteins and viral proteins VPg-Pro and CI. A) Schematic representation of the HCPro purification procedure. The workflow includes systemic infection of *N. benthamiana* plants with recombinant PVA expressing HCPro fused to two copies of the Strep tag (2xStrep) and RFP, binding of the fusion protein and its associated proteins to the Strep-Tactin resin, washing away of unbound proteins, elution of the protein complexes with biotin and their analysis by LC-MS/MS. Selected HCPro binding partners identified by LC-MS/MS are listed in the table below. B) Validation of the HCPro(2xStrep)-RFP purification procedure by Western blotting. Three independent biological replicates of HCPro(2xStrep)-RFP purification were analyzed in parallel with three purification controls from plants infected with the wild type virus having no affinity tags in the polyprotein sequence. The control lane (ctrl) represents a total lysate of cells infected with PVA-HCPro(2xStrep)-RFP. C) Validation of the selected HCPro binding partners by Western blotting. Purified HCPro complexes were analyzed as in (B) with antibodies against VPg, CI and S-adenosyl-L-methionine synthase 1 (SAMS1). Arrowheads indicate the positions of monomeric proteins.

Western blots were deliberately overexposed to confirm the absence of signal in the controls. The positions of molecular mass markers are shown in kDa on the left of each panel.
231x319mm (300 x 300 DPI)

CONFIDENTIAL

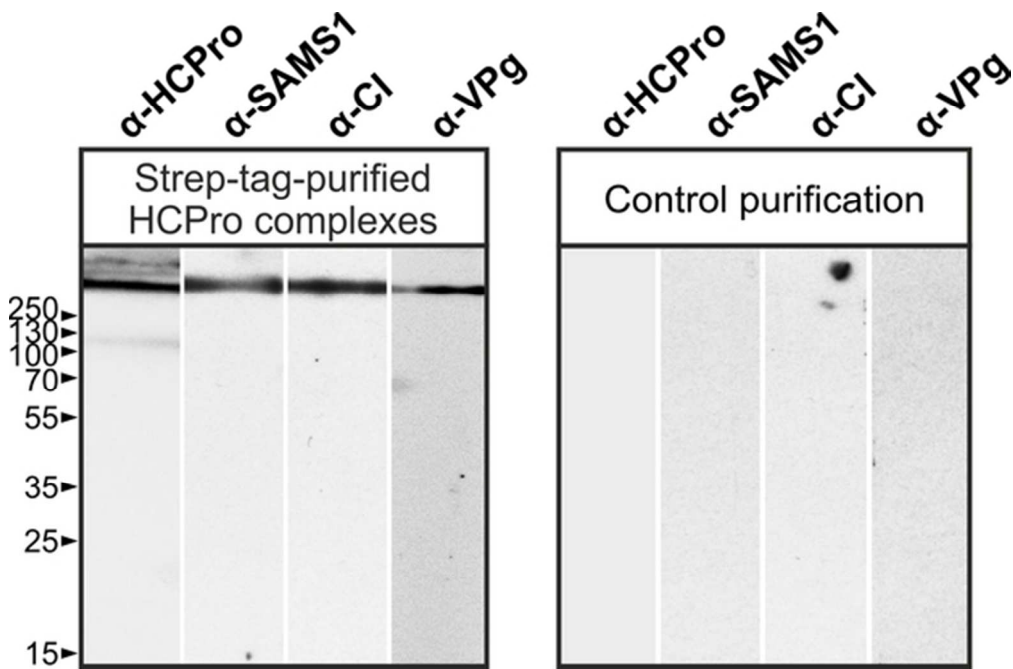


Figure 2. Large multiprotein complexes formed by HCPPro in systemically infected plants simultaneously contain SAMS, CI, AGO1 and VPg (VPg-Pro). Protein sample purified as described in Fig. 1 was separated by SDS-PAGE on a single wide lane and transferred to a blotting membrane. The membrane was cut into equal strips and probed with antibodies against HC-Pro, SAMS1, CI, AGO1 or VPg. Note that all antibodies recognized a band of the same electrophoretic mobility. The positions of molecular mass markers are shown in kDa on the left.

52x34mm (300 x 300 DPI)

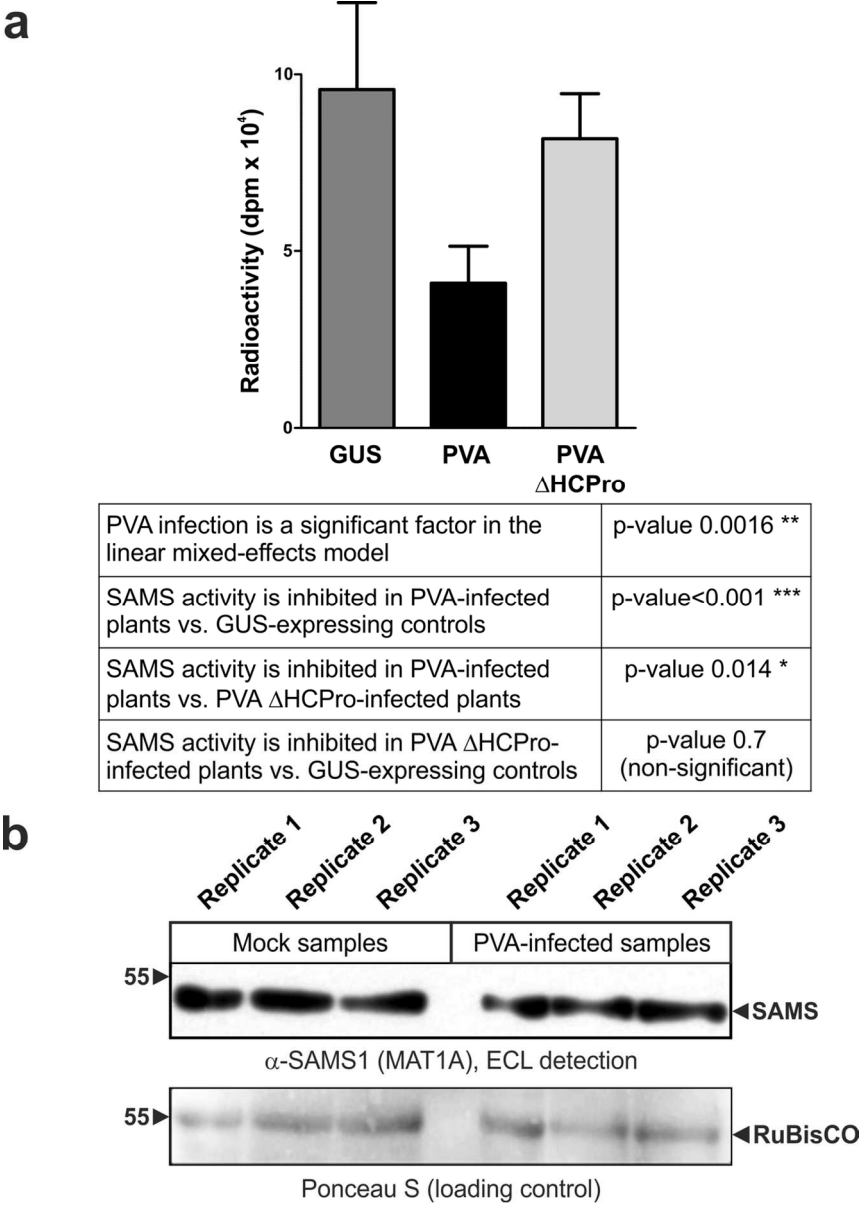


Figure 3. PVA infection inhibits SAMS enzymatic activity whereas PVA ΔHCPPro expression doesn't. A) *N. benthamiana* leaves were infiltrated with *A. tumefaciens* strains carrying cDNA of PVA (PVA), cDNA of PVA lacking the HCPPro sequence (PVA ΔHCPPro) or a control vector expressing an irrelevant β-glucuronidase gene (GUS). At 5 days post-infiltration, total SAMS enzymatic activity was assayed in leaf extracts by measuring the radioactivity incorporated into SAM from 35S-labeled L-methionine (Met) in the presence of ATP. Prior to radioactivity measurements, 35S-labeled SAM was separated from 35S-Met using phosphocellulose cation exchange paper. Background subtraction was carried out as described in Fig. S2. Two independent experiments were carried out with two or three biological replicates, each of which was technically replicated three times. Data from one representative experiment is shown as a bar graph. The bars represent means of three biological replicates ± standard error of the mean (SEM). A linear mixed-effects model, in which replication is treated as a random effect, was applied to examine whether SAMS enzymatic activity was affected by PVA infection. The table shows the results of statistical analysis using the mixed-effects model. The following significance codes are used: *** (<0.001), ** (<0.01), * (<0.05). B) The inhibition of SAMS

1
2
3
4
5
6
7
8
9
10
11
12
13
14
15
16
17
18
19
20
21
22
23
24
25
26
27
28
29
30
31
32
33
34
35
36
37
38
39
40
41
42
43
44
45
46
47
48
49
50
51
52
53
54
55
56
57
58
59
60

activity in PVA-infected plants is not due to SAMS degradation. Upper panel: comparison of SAMS protein levels in mock- and PVA-infected cells by Western blotting. Lower panel: loading control showing Ponceau S-stained RuBisCO band on the blotting membrane.
112x157mm (300 x 300 DPI)

CONFIDENTIAL

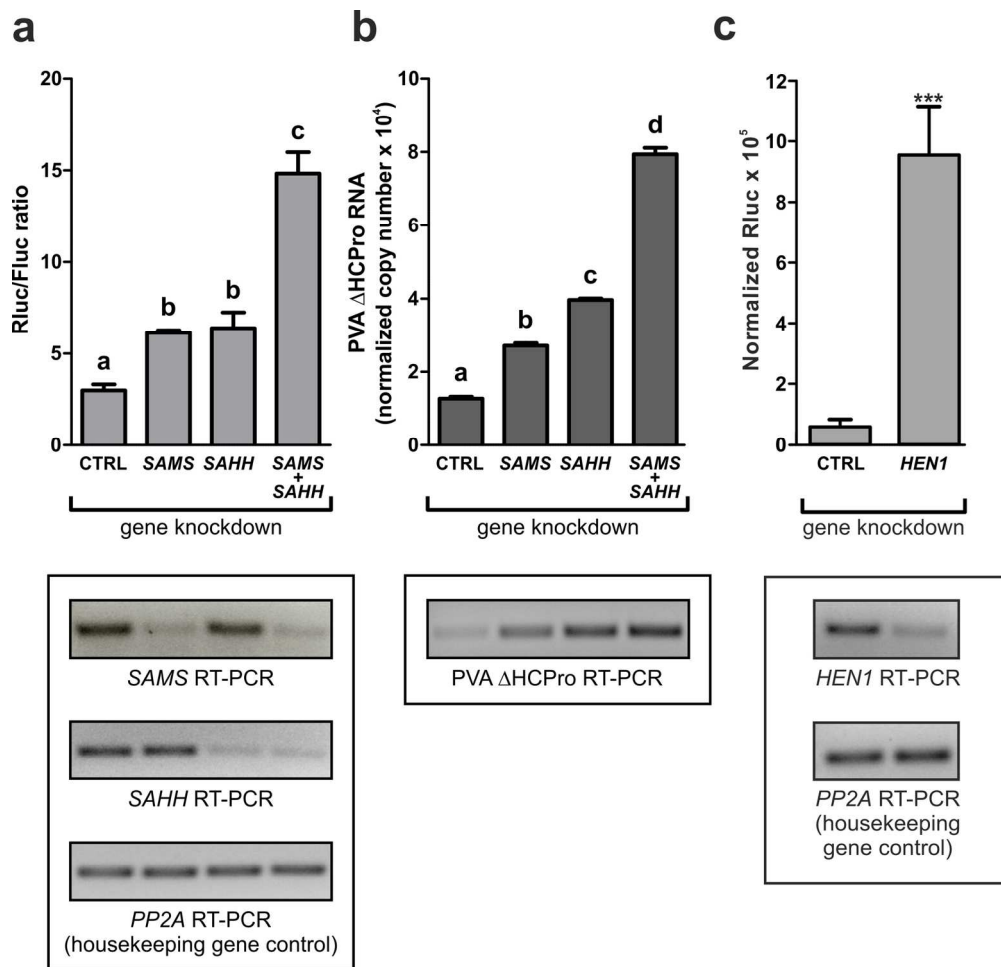


Figure 4. Partial rescue of the HCPPro-deficient PVA phenotype by SAMS, SAHH and HEN1 knockdown. *N. benthamiana* leaves were co-infiltrated with *Agrobacterium* strains carrying cDNA of PVA lacking HCPPro (PVA Δ HCPPro) and expressing Renilla luciferase, a control reporter vector constitutively expressing Firefly luciferase and a silencing vector expressing hairpin RNAs targeting SAMS, SAHH or HEN1. In the negative control (CTRL), leaves were infiltrated with the same *Agrobacterium* strains, except that the silencing vector lacked any RNA hairpin sequence. SAMS, SAHH and HEN1 knockdown was confirmed by RT-PCR. A) Rluc activity was measured at 5 days post-inoculation and normalized to the Fluc activity. Note the increase in the normalized viral gene expression induced by the knockdown of SAMS or SAHH and the synergistic effect exhibited by the knockdown of both genes. The absolute luminescence values are presented in supplementary Fig. S4. B) PVA Δ HCPPro RNA copy numbers were quantified in the samples by RT-PCR and normalized to expression of a housekeeping gene (PP2A). Note the accumulation of viral RNA upon SAMS or SAHH knockdown. C) Rluc activity was measured at 5 days post-inoculation and normalized to the Fluc activity. Note the accumulation of Rluc upon HEN1 knockdown. Data are represented as means of five (A) or six (B) and (C) biological replicates \pm standard error of the mean (SEM). Different letters above bars in (A) and (B) indicate significant differences (t-test, $p < 0.05$). The same letter indicates no significant difference (t-test, $p > 0.1$). *** denotes statistical significance ($p < 0.001$) in (C).

161x155mm (300 x 300 DPI)

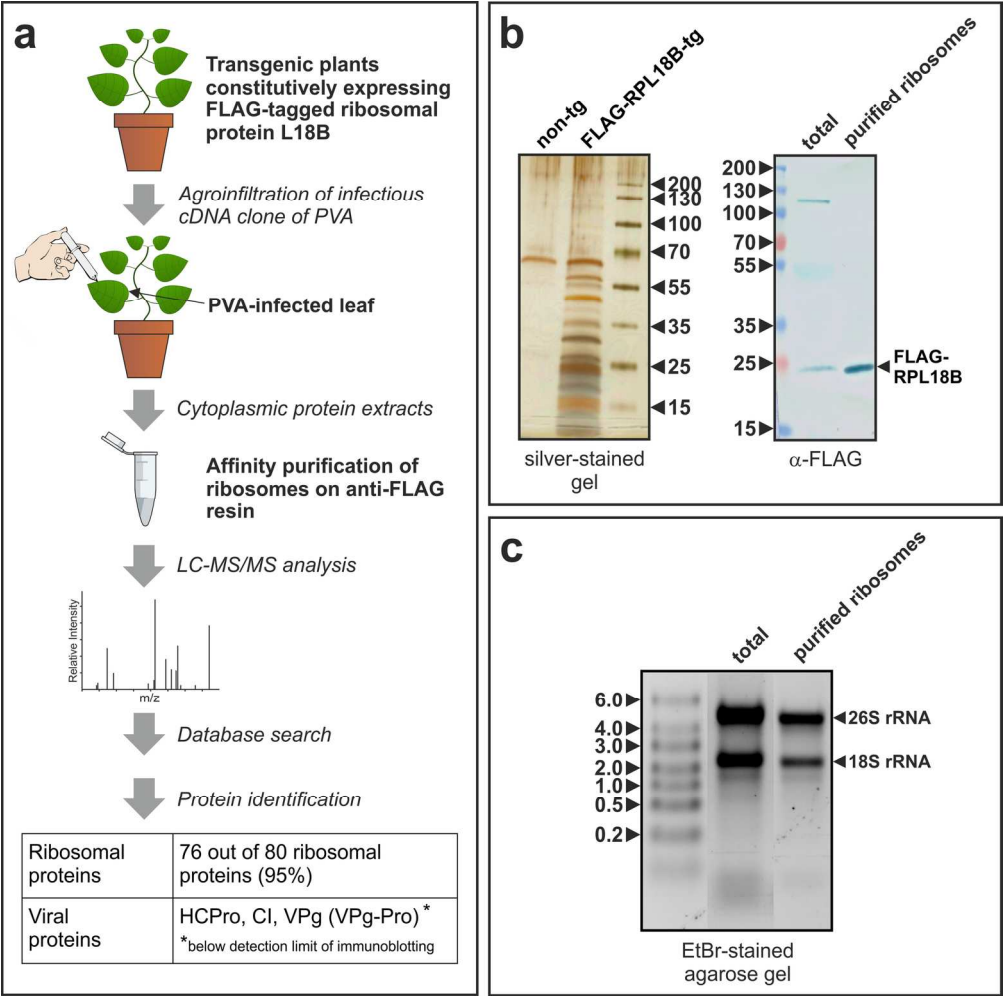


Figure 5. HCPPro, CI and VPg are bound to ribosomes in PVA-infected cells. A) Schematic representation of the ribosome purification procedure. Transgenic *N. benthamiana* plants constitutively expressing the FLAG-tagged large subunit ribosomal protein L18B from *A. thaliana* were infected with PVA through agroinfiltration. Ribosomes were purified from cytoplasmic extracts of infected leaves using anti-FLAG immunoaffinity resin at 4 days post-infiltration. Purified ribosomes were analyzed by LC-MS/MS for the presence of associated viral proteins. Samples from PVA-infected non-transgenic plants were used as purification controls. B) Validation of the ribosome purification procedure by SDS-PAGE/silver-staining (left panel) and Western blotting with anti-FLAG antibody (right panel). Note the detection of characteristic low molecular weight proteins in samples purified from transgenic (tg) plants, but not in purifications from non-transgenic (non-tg) controls. The positions of molecular mass markers are shown in kDa. C) Validation of the ribosome quality and integrity by means of electrophoretic analysis of ribosomal RNA (rRNA). Note the similar rRNA integrity and ratio between 26S and 18S rRNA in the purified ribosomes and the total RNA sample. The positions of molecular mass markers are shown on the left in kilobases.

166x165mm (300 x 300 DPI)

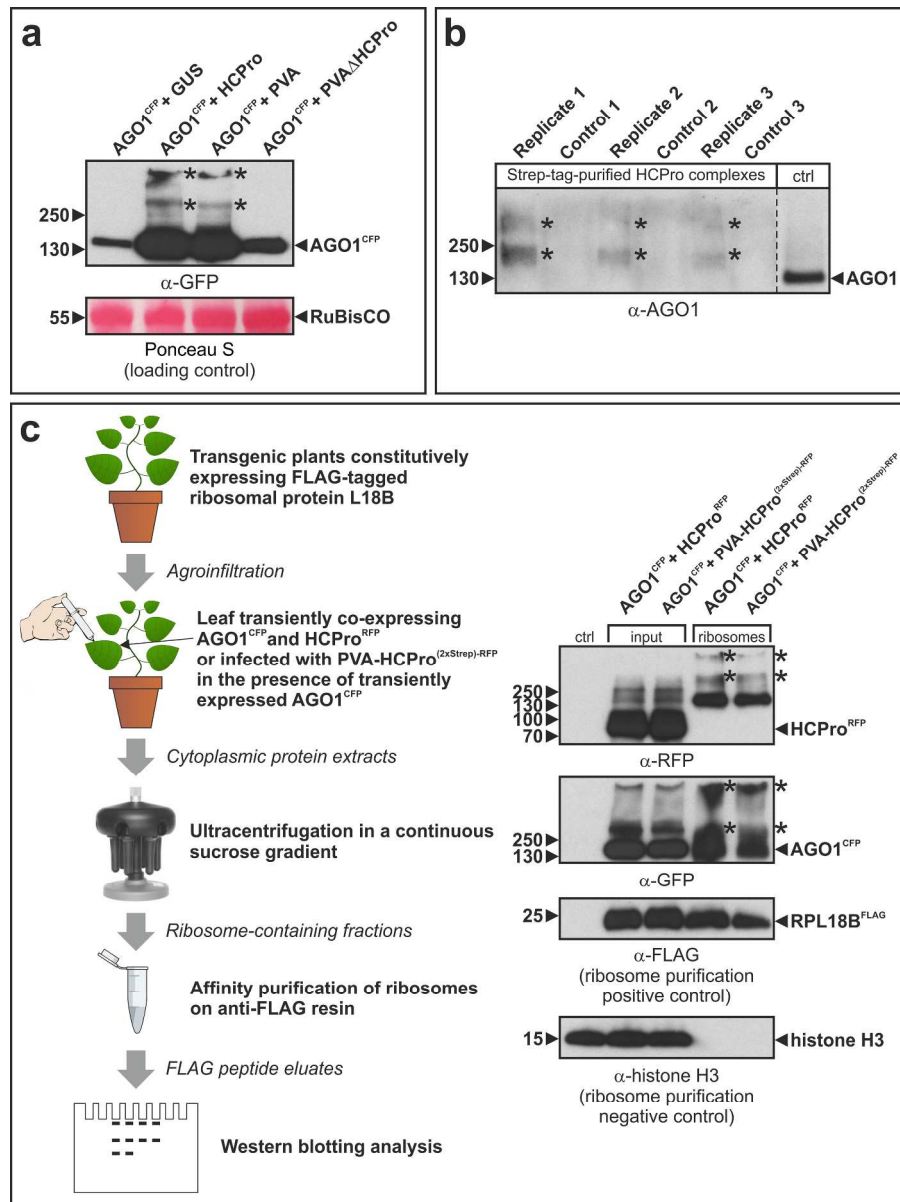


Figure 6. RNA silencing suppressor HCPPro and AGO1, the core component of RISC, interact with each other and are both associated with ribosomes. A) AGO1 and HCPPro form stable complexes in planta. The panel shows Western blot analysis of total lysates from cells co-expressing AGO1^{CFP} and HCPPro. *N. benthamiana* leaves were infiltrated with *A. tumefaciens* carrying AGO1^{CFP} and HCPPro or AGO1^{CFP} and a full-length infectious cDNA clone of PVA. In the negative controls, AGO1^{CFP} was co-expressed with an unrelated bacterial protein β -glucuronidase (GUS) or PVA lacking HCPPro (PVA Δ HCPPro). Note the formation of AGO1^{CFP} complexes in the presence of HCPPro, but not in the controls. B) Endogenous AGO1 binds to HCPPro in systemically infected *N. benthamiana* plants. Strep-tag-purified HCPPro complexes (see Figure 1) were analyzed by Western blotting with anti-AGO1 antibody. Note the pull-down of AGO1 complexes with HCPPro(2xStrep)-RFP in all purification replicates, but not in the controls. C) HCPPro and AGO1 are both associated with ribosomes. Transgenic plants constitutively expressing FLAG-tagged ribosomal protein L18B were infiltrated with *A. tumefaciens* carrying AGO1^{CFP} and HCPPro^{RFP} or AGO1^{CFP} and PVA-HCPPro(2xStrep)-RFP. Ribosomes were purified in a two-step procedure involving ultracentrifugation in a continuous sucrose

gradient followed by affinity purification on anti-FLAG resin. Purified ribosomes were analyzed by Western blotting for the presence of associated HCPProRFP and AGO1CFP. A sample from non-transgenic *N. benthamiana* was used as a negative control (left lane). Arrowheads indicate the positions of monomeric proteins and asterisks indicate the positions of putative HCPPro-AGO1 complexes. The positions of molecular mass markers are shown in kDa on the left of each panel.

224x299mm (300 x 300 DPI)

CONFIDENTIAL

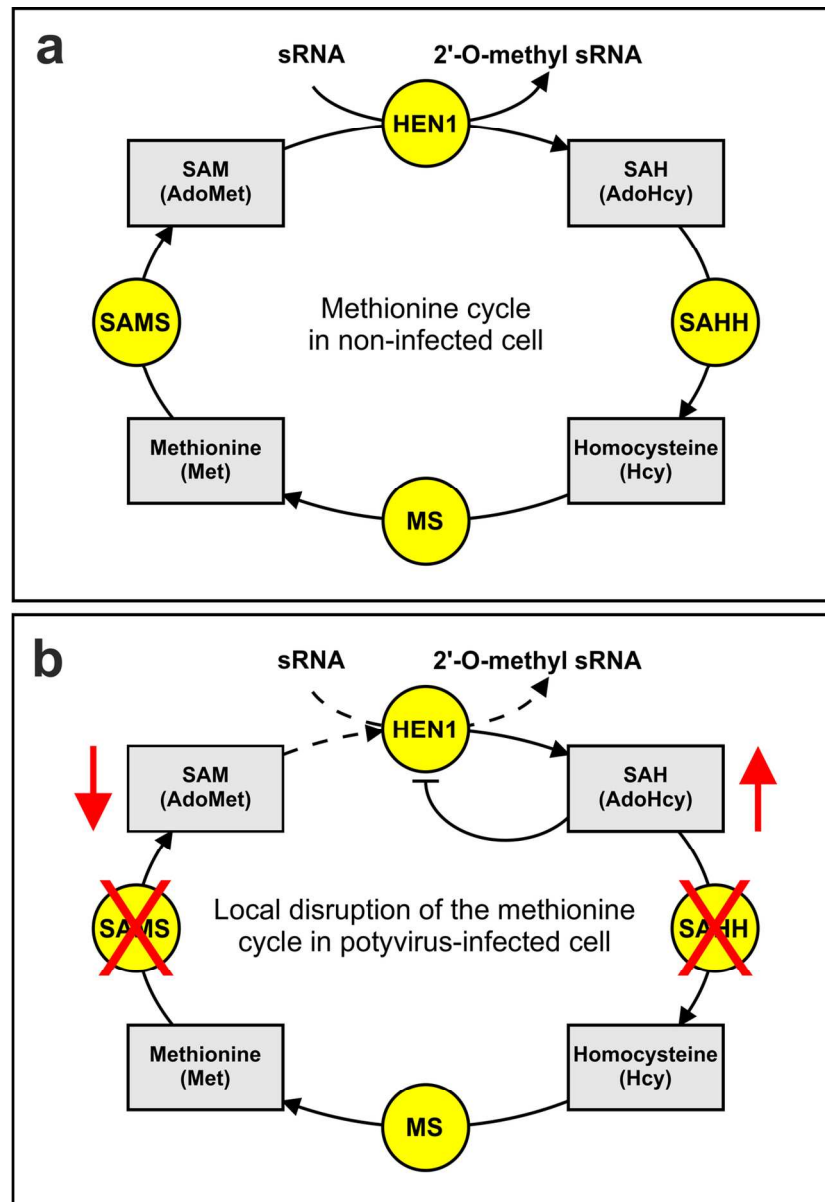


Figure 7. Hypothetical model for the suppression of antiviral RNA silencing through local disruption of the methionine cycle. A) Schematic representation of the methionine cycle in non-infected cells. SAMS catalyzes the conversion of methionine to SAM, which serves as a methyl donor for HEN1. HEN1 methylates sRNAs, protecting them from degradation before their loading onto RISC. The methylation reaction byproduct SAH is subsequently broken down by SAHH to homocysteine, which is recycled back to methionine by MS. B) In potyvirus-infected cells, HCPro acts together with other viral proteins to locally inhibit SAMS and SAHH. As a result, HEN1 is deprived of its substrate SAM and poisoned by its feedback inhibitor SAH. This, in turn, leads to the inhibition of sRNA methylation and suppression of RNA silencing via sRNA polyuridylation and degradation. Circles represent enzymes and grey rectangles represent small molecules. Falling levels of SAM and rising levels of SAH are indicated by arrows. SAM: S-adenosyl-L-methionine; SAMS: S-adenosyl-L-methionine synthase; HEN1: HUA ENHANCER 1; SAH: S-adenosyl-L-homocysteine; SAHH: S-adenosyl-L-homocysteine hydrolase; MS: methionine synthase.

115x167mm (300 x 300 DPI)

1
2
3
4
5
6
7
8
9
10
11
12
13
14
15
16
17
18
19
20
21
22
23
24
25
26
27
28
29
30
31
32
33
34
35
36
37
38
39
40
41
42
43
44
45
46
47
48
49
50
51
52
53
54
55
56
57
58
59
60

CONFIDENTIAL

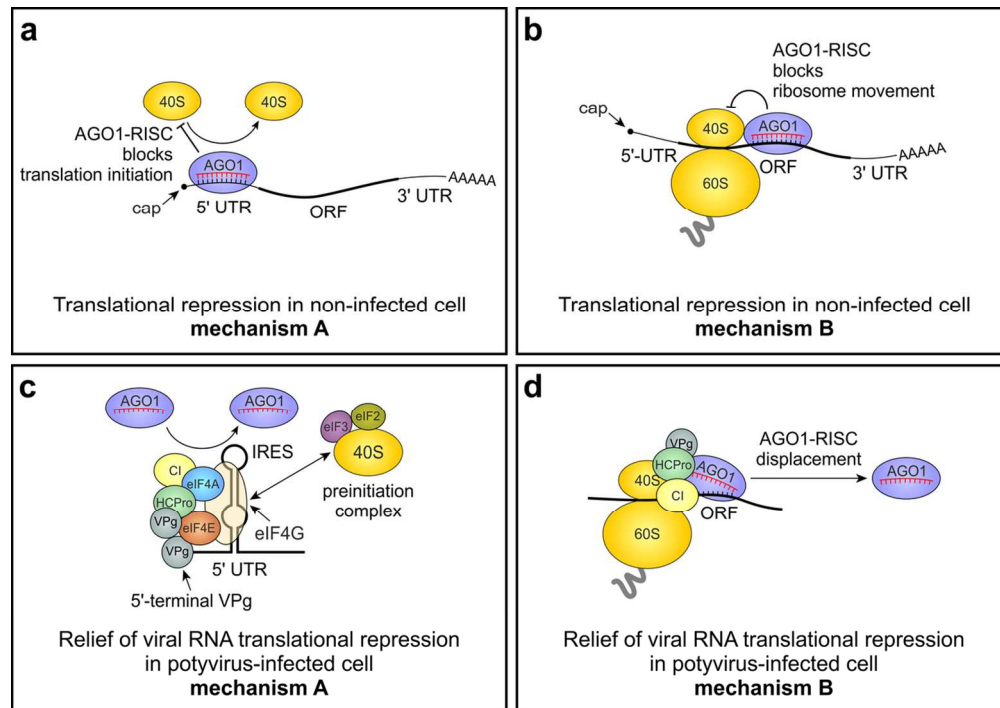


Figure 8. Hypothetical model for the relief of antiviral translational repression in potyvirus-infected cells. A-B) Putative plant-specific mechanisms of RISC-mediated translational repression. sRNAs that are highly complementary to their targets in the 5' UTR or ORF are incorporated into AGO1-RISC to repress mRNA translation either by inhibiting the initiation (A) or by sterically hindering ribosome movement (B) (Iwakawa and Tomari, 2013). The mechanism responsible for the inhibition of translation initiation may involve the AGO1-RISC-induced dissociation of the DExD/H-box helicase eIF4A from target mRNA and/or steric hindrance of 40S ribosomal subunit binding to the mRNA. C-D) In potyvirus-infected cells, HCPro may act together with CI and VPg/VPg-Pro to relieve translational repression of viral RNA. During the IRES-mediated initiation (C), virus-specific protein complexes could be formed with eIF4A, preventing the AGO1-RISC-induced dissociation of eIF4A (Fukao et al. 2014, Fukaya et al. 2014) from viral RNA. This allows the recruitment of preinitiation complexes to the IRES-bound eIF4F complex and subsequent initiation of translation. During this process, the viral DExD/H-box helicase CI might act as an RNP remodeling factor functionally assisting the initiation of translation. Although the direct involvement of the cap-binding protein eIF4E in the cap-independent initiation of potyviral RNA translation remains uncertain, the interaction of eIF4E with HCPro and VPg could assist the relief of viral RNA translational repression. Free VPg or its precursor VPg-Pro could be targeted to the eIF4F complex through interaction with eIF4E and/or dimerization with the VPg covalently attached to the 5' end of viral RNA. During translation elongation (D), viral proteins associated with ribosomes may induce the displacement of AGO1-RISC from viral RNA. The putative RNP remodeling activity of CI might play a role in this process, assisting the intrinsic ability of the ribosome to displace RNA-bound proteins in its path.

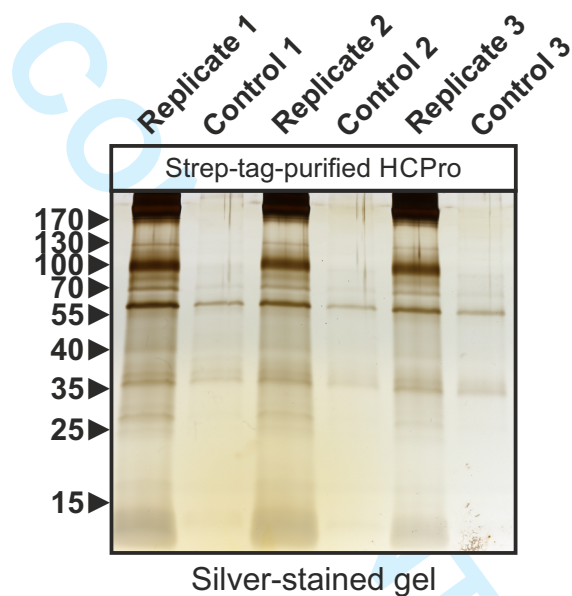
118x83mm (300 x 300 DPI)

1
2
3
4
5
6
7
8
9
10
11
12
13
14
15
16
17
18
19
20
21
22
23
24
25
26
27
28
29
30
31
32
33
34
35
36
37
38
39
40
41
42
43
44
45
46
47
48
49
50
51
52
53
54
55
56
57
58
59
60

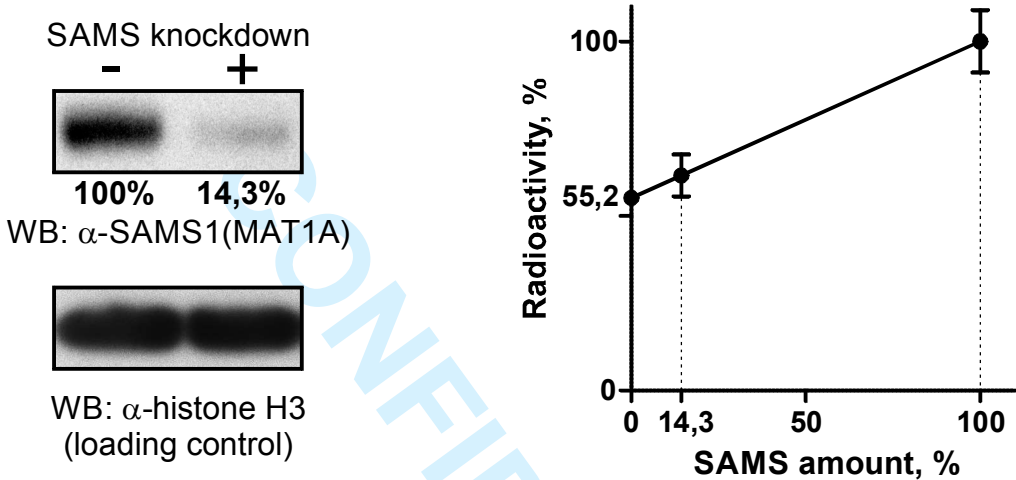
Supplementary Table S1 Recombinant constructs used in this study.

Construct name	Gene Cassette	Vector	Description	Ref.
PVA	35S-PVA ^{wt} :: <i>rluc</i> ^{int} -nos	pRD400	Rluc-tagged full-length infectious cDNA clone of PVA	(Eskelin et al., 2010)
PVA ΔHCPPro	35S-PVA-ΔHCPPro:: <i>rluc</i> ^{int} -nos	pRD400	Rluc-tagged PVA lacking HCPPro	*
PVA-HCPPro ^(2xStrep) -RFP	35S-PVA-[(2xStrep)-RFP-HCPPro]:: <i>rluc</i> ^{int} -nos	pRD400	Rluc-tagged PVA expressing HCPPro fused to the red fluorescent protein (RFP) and two copies of the Strep-tag II	*
HCPPro	35S-HCPPro-nos	pRD400	Plasmid constitutively expressing PVA HCPPro	*
HCPPro ^{RFP}	2x35S-RFP-HCPPro-T35S	pSITEII-6C1	Plasmid constitutively expressing PVA HCPPro fused to RFP	*
AGO1 ^{CFP}	2x35S-CFP-AGO1-T35S	pSITEII-2C1	Plasmid constitutively expressing <i>N. benthamiana</i> AGO1 fused to CFP	*
Fluc ^{int}	35S- <i>fluc</i> ^{int} -nos	pRD400	Plasmid constitutively expressing intron-spliced <i>Fluc</i>	*
GUS	35S-GUS-nos	pRD400	Plasmid constitutively expressing <i>uidA</i> gene encoding β-glucuronidase (GUS)	(Eskelin et al., 2011)
pHG SAMS	35S-SAMS(hp)-ocs	pHELLS GATE 12	Plasmid constitutively expressing hairpin RNA targeting the SAMS gene family	This study
pHG SAHH	35S-SAHH(hp)-ocs	pHELLS GATE 12	Plasmid constitutively expressing hairpin RNA targeting the SAHH gene family	This study
pHG HEN1	35S-HEN1(hp)-ocs	pHELLS GATE 12	Plasmid constitutively expressing hairpin RNA targeting the HEN1 gene family	This study

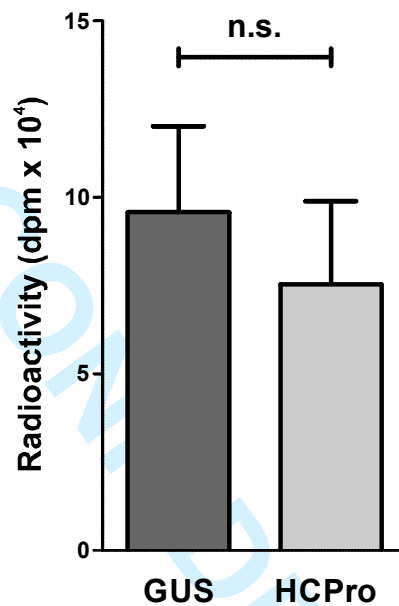
* Hafrén et al., submitted



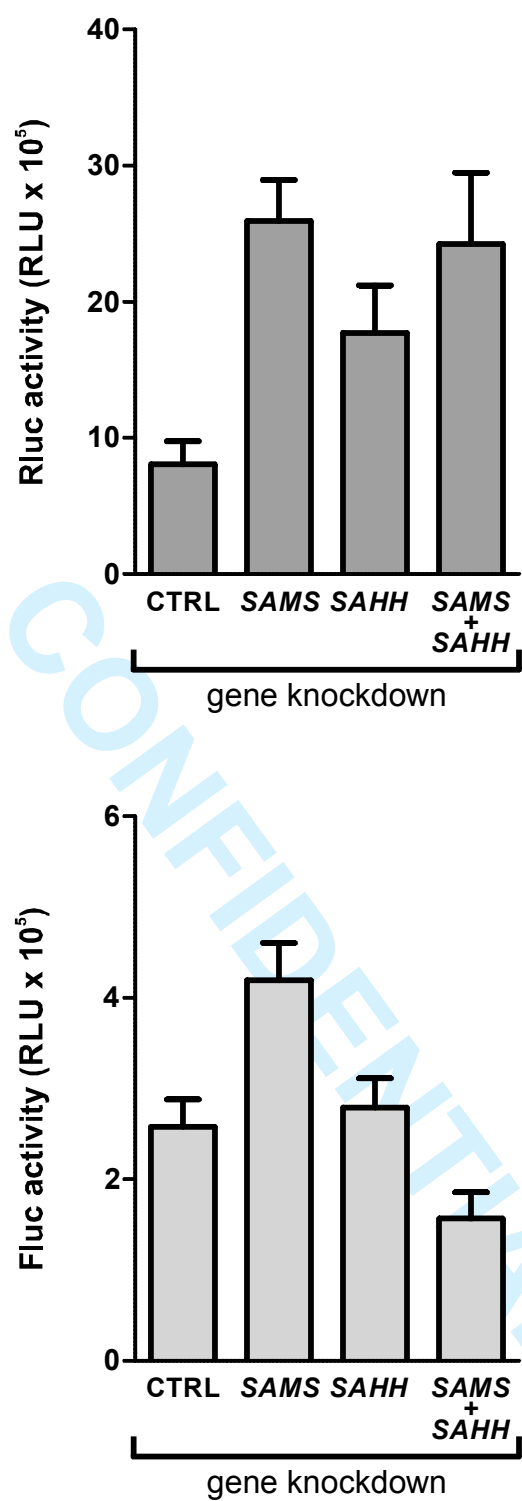
Supplementary Figure S1. Analysis of affinity-purified HCPro complexes by SDS-PAGE and silver staining. Strep-tag purification was carried out as schematically represented in Fig.1. Equal sample volumes were loaded onto each lane. Note the difference in protein content between the purified HCPro^{(2xStrep)-RFP} complexes and control samples.



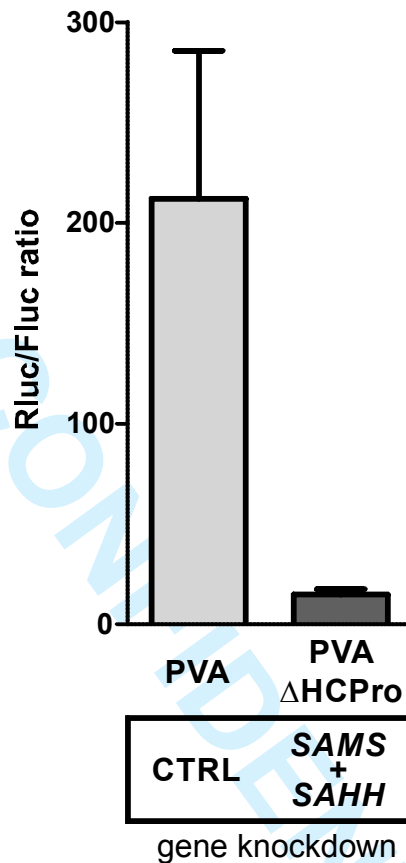
Supplementary Figure S2. The use of SAMS knockdown for background subtraction in SAMS activity assays. All known members of the SAMS gene family were transiently silenced in *N. benthamiana* leaves using a silencing vector producing the corresponding intron-spliced hairpin RNA. The same vector without an insert was used in the negative control (-). At 7 days post silencing, SAMS protein levels were assayed by Western blotting with a pan anti-SAMS antibody, followed by protein band densitometry (upper left panel). SAMS enzymatic activity was assayed in the samples by measuring the radioactivity incorporated into SAM from ³⁵S-labeled L-methionine (Met) in the presence of ATP. Control reactions contained all reagents except for ATP. Each assay comprised three biological replicates, each of which was technically replicated three times. Prior to radioactivity measurements, ³⁵S-labeled SAM was separated from ³⁵S-Met using phosphocellulose cation exchange paper. A standard curve of SAMS amount versus measured radioactivity allowed us to determine that ~55% of radioactivity retained on phosphocellulose corresponded to products of non-specific reactions involving ³⁵S-Met and ATP. Error bars represent standard deviation (SD).



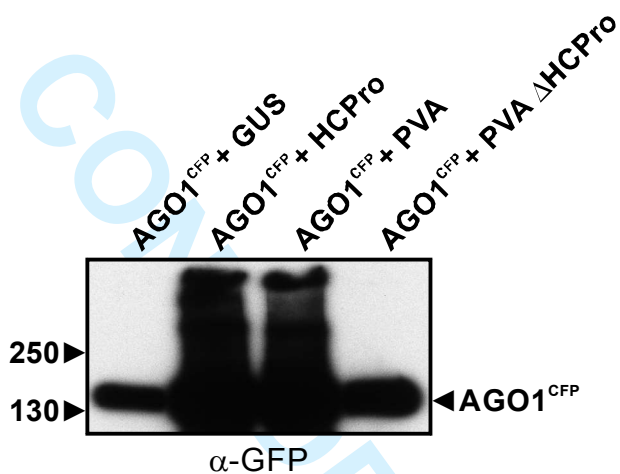
Supplementary Figure S3. HCPPro, when expressed alone, is unable to inhibit the enzymatic activity of SAMS. *N. benthamiana* leaves were agroinfiltrated with *A. tumefaciens* strains carrying vectors expressing HCPPro or the β -glucuronidase control gene (GUS). At 5 days post agroinfiltration, SAMS enzymatic activity was assayed by measuring the radioactivity incorporated into SAM from ^{35}S -labeled L-methionine (Met) in the presence of ATP. Control reactions contained all reagents except for ATP. Prior to radioactivity measurements, ^{35}S -labeled SAM was separated from ^{35}S -Met using phosphocellulose cation exchange paper. Background subtraction was carried out as described in Fig. S2. Each assay comprised three biological replicates, each of which was technically replicated three times. Data are represented as means \pm standard error of the mean (SEM). n.s. indicates statistically non-significant differences (t-test, $p > 0.1$).



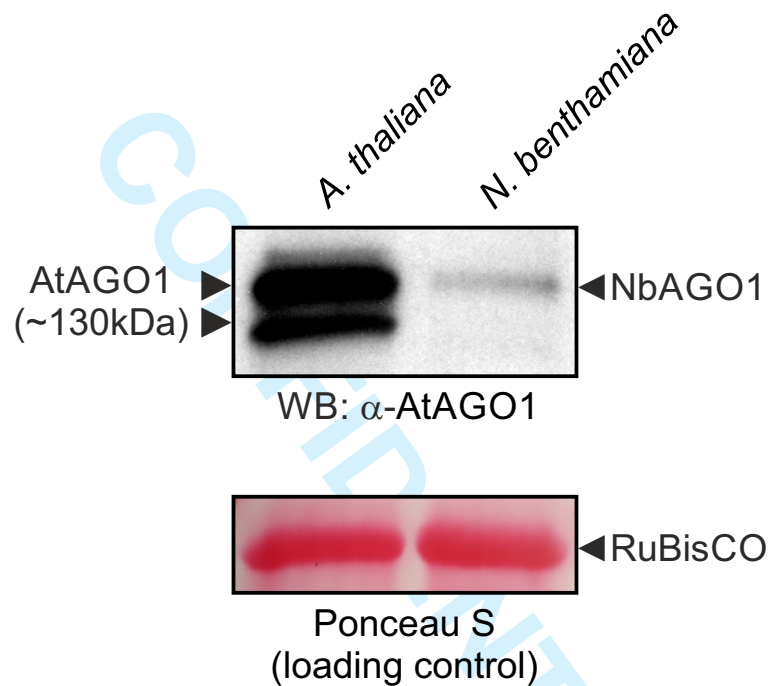
Supplementary Figure S4. Light emitted by the Rluc- and Fluc-catalyzed bioluminescent reactions (in relative light units; RLU), measured in the experiments shown in Fig. 3. Note that simultaneous knockdown of *SAMS* and *SAHH* decreased the plasmid-driven Fluc expression. This was likely due to a stronger inhibition of various cellular methylation-dependent processes compared to the individual knockdown. Such inhibition could overpower the positive effect of the knockdown on Fluc expression due to suppression of Fluc silencing. The virus-driven Rluc expression was not similarly decreased (upper panel), indicating that the effect of the knockdown on reporter expression was virus-specific. Data are means of 5 biological replicates \pm standard error of the mean (SEM).



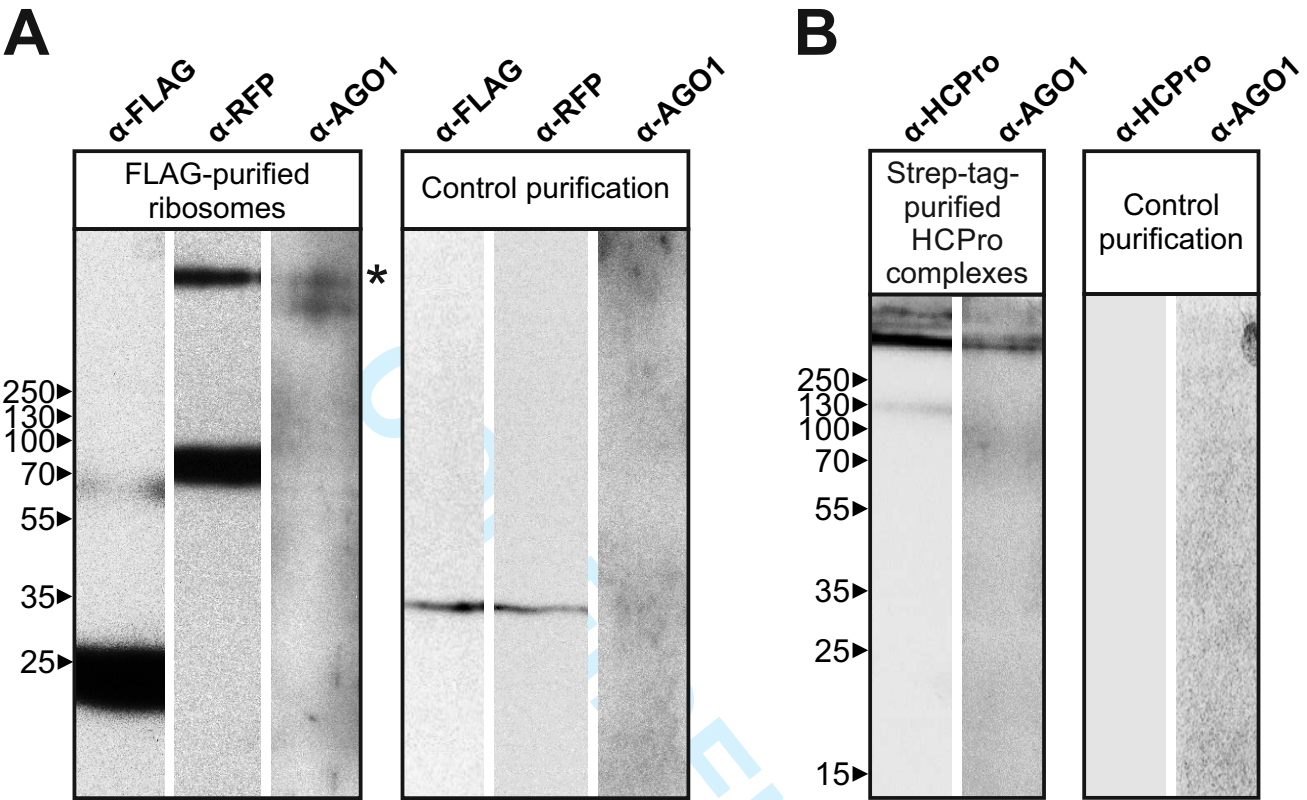
Supplementary Figure S5. SAMS and SAHH knockdown can only partially rescue the loss of HCPPro in PVA. In the left experiment, *N. benthamiana* leaves were co-infiltrated with *Agrobacterium* strains carrying cDNA of PVA (PVA) expressing *Renilla* luciferase, a control reporter vector constitutively expressing Firefly luciferase (Fluc^{int}) and a control silencing vector (CTRL) lacking RNA hairpin sequence. In the right experiment, leaves were co-infiltrated with *Agrobacterium* strains carrying cDNA of PVA lacking HCPPro (PVA Δ HCPPro) and expressing *Renilla* luciferase, Fluc^{int} and the silencing vector expressing hairpin RNAs targeting SAMS or SAHH. Rluc and Fluc activities were measured at 5 days post-inoculation. More than 15-fold difference in the Rluc/Fluc activity ratio between the experiments shows that the rescue of the HCPPro-deficient PVA phenotype by the SAMS and SAHH knockdown was only partial. This was likely due to the inability of the knockdown to compensate for the loss of multiple HCPPro functions unrelated to inhibition of the methionine cycle. Data are represented as means \pm standard error of the mean (SEM).



Supplementary Figure S6. Overexposed image of the anti-GFP Western blot from Figure 5A. Note the complete absence of bands corresponding to heavy molecular weight complexes in the controls (left and right lanes).



Supplementary Figure S7. Rabbit polyclonal antibody against the N-terminal peptide of *A. thaliana* AGO1 (AtAGO1) recognizes AGO1 from *N. benthamiana* (NbAGO1). Total lysates of *A. thaliana* and *N. benthamiana* leaves were analyzed by Western blotting (WB) using the anti-AtAGO1 antibody. Equal loading was controlled by staining the membrane with Ponceau S.



Supplementary Figure S8. Detection of HCPPro and AGO1 in large protein complexes from virus-infected plants. A) Ribosomes were purified using anti-FLAG affinity gel from the FLAG-RPL18B transgenic plants infected with PVA expressing RFP-tagged HCPPro. Purified ribosome sample was separated by SDS-PAGE on a single wide lane and transferred to a blotting membrane. The membrane was cut into equal strips and probed with antibodies against the FLAG tag, RFP and AGO1. Note that the upper band recognized by the anti-AGO1 antibody (marked by an asterisk) corresponds in size to the HCPPro-specific band recognized by the RFP antibody. Mock-purified sample from virus-infected non-transgenic plants was used as a negative control. B) HCPPro^{(2xStrep)-RFP} complexes purified as described in Fig. 1 were analyzed by Western blotting as in (A) using antibodies against HCPPro and AGO1. Note that both antibodies recognized a band of the same electrophoretic mobility. Mock-purified sample from plants infected with untagged HCPPro was used as a negative control. The positions of molecular mass markers are shown in kDa on the left of each panel.

Supplementary Methods

Antibodies

Commercial primary antibodies used in this study include the following: mouse monoclonal anti-RFP (SignalChem, Canada), rabbit polyclonal anti-MAT1A (ProteinTech, USA-China), rabbit polyclonal anti-AtAGO1 (Agrisera, Sweden), rabbit polyclonal anti-histone H3 (Cell Signaling Technology, USA), mouse monoclonal anti-FLAG M2-peroxidase (Sigma-Aldrich, USA), mouse monoclonal anti-GFP (B-2; Santa Cruz Biotechnology, USA). Polyclonal anti-CI and anti-VPg antibodies have been produced in-house through immunization of rabbits with purified recombinant proteins expressed in *E. coli*. The horseradish peroxidase (HRP)-conjugated secondary antibodies used for Western blot analysis were from Promega (USA).

Agroinfiltration

A. tumefaciens were transformed with binary vector constructs by electroporation. The bacterial cells were grown in LB medium for 1-3 hours at 28°C with shaking and plated on LB plates containing appropriate antibiotics. Selected colonies were grown overnight at 28°C with shaking in LBMA medium (LB medium supplemented with 10 mM MES (pH 6.3), 20 µM acetosyringone and appropriate antibiotics). The overnight cultures were diluted ~1:10 in the same medium and grown at 28°C with shaking until the OD₆₀₀ value is in the range of 0.7-1.5. Cells were harvested by centrifugation at 3500g for 10 min at room temperature, washed twice with induction buffer (10 mM MES (pH 6.3), 10 mM MgCl₂ and 150 µM acetosyringone) and re-suspended in induction buffer. OD₆₀₀ of cell suspensions was measured with an Eppendorf BioPhotometer and cell density was adjusted to the desired value with induction buffer. Cell suspensions were incubated for 2 h at room temperature prior to leaf infiltration. Young *N. benthamiana* plants were selected for agroinfiltration based on size and uniformity. Infiltration was carried out by carefully turning the leaf upside down and gently injecting the bacterial suspension with a 1 ml syringe. The plants were sampled at various time points post-infiltration by cutting 5–10 mm leaf discs with a cork borer. The disks were frozen immediately in liquid nitrogen and stored at -70°C.

Liquid chromatography-tandem mass spectrometry (LC-MS/MS)

Disulfide bridges in proteins were reduced with 50mM TCEP (Tris(2-carboxyethyl)phosphine hydrochloride salt, Sigma-Aldrich, USA) for 20 min at 37°C. To block cysteine residues, iodoacetamide (Fluka, Sigma-Aldrich, USA) was added to a final concentration of 50 mM and the

samples were incubated at room temperature in the dark for 30 min. A total of 1 µg trypsin (Sequencing Grade Modified Trypsin, Promega) was added, and the samples were incubated overnight at 37°C. Tryptic digests were quenched with 10% (v/v) trifluoroacetic acid (TFA) and purified using C18 microspin columns (Harvard Apparatus, USA). Columns were eluted with 0.1% (v/v) TFA in 50% (v/v) acetonitrile (ACN) and the volume of the eluted samples was reduced to approximately 2 µl in a vacuum centrifuge. The peptides were reconstituted to a final volume of 30 µl with 0.1% (v/v) TFA, 1% (v/v) ACN and vortexed thoroughly. LC-MS/MS analysis was carried out using an EASY-nLC nano-HPLC system (Thermo Scientific, Germany) connected to a Velos Pro-Orbitrap Elite hybrid mass spectrometer (Thermo Fisher Scientific, Germany) with a nano-electrospray ion source (Thermo Scientific, Germany). A two-column setup was used, consisting of a 2 cm C18-A1 trap column (Thermo Scientific, Germany), followed by a 10 cm C18-A2 analytical column (Thermo Scientific, Germany). Linear separation gradient was 5% (v/v) buffer B (0.1% fluoroacetic acid in 98% ACN) in 5 min, 35% (v/v) buffer B in 60 min, 80% (v/v) buffer B in 5 min and 100% buffer B in 10 min at a flow rate of 0.3 µl/min. 4 µl of sample was injected per LC-MS/MS run. Full MS scan was acquired with a resolution of 60,000 over a normal mass range of the Orbitrap analyzer; the method was set to fragment the 20 most intense precursor ions with CID (energy 35). Data was acquired using Xcalibur software (version 2.7.1). Acquired MS2 scans were searched against the *N. benthamiana* annotated protein database derived from solgenomics.net using the SEQUEST search algorithm in the Proteome Discoverer software (Thermo Fisher Scientific, Germany). Allowed mass error was 15 ppm for precursor ions and 0.8 Da for fragment ions. Carbamidomethylation (+57.021 Da) of cysteine was set as a static modification and oxidation of methionine (+15.995 Da) as a dynamic modification. Database searches were limited to fully tryptic peptides with maximum one missed cleavage.

SAMS, SAHH and HEN1 knockdown experiments

PCR fragments corresponding to conserved regions within the SAMS, SAHH and HEN1 gene families were designed using Primer3 Plus software (Untergasser *et al.* 2012). The primer sequences were as follows: SAMS, 5'-ACGCCCCGAGTTGATGCCTCTTAGTC-3' and 5'-ACCTCCATGAGCACCCACCTCCG-3'; SAHH, 5'-TTGATGATGGTGGTGATGCT-3' and 5'-ACCATCGGGAAGTGAGTGAC-3'; HEN1, 5'-GCCAGCATCGATTATCTGAAC-3' and 5'-ATCATGTCAATTCTTGCCCA-3'. The number of targeted gene family members was 4 for SAMS, 7 for SAHH and 2 for HEN1. The obtained PCR fragments were inserted into pGEM-T Easy vector (Promega, USA) and then recombined into pHELLSGATE 12 silencing vector (CSIRO Plant Industry, Australia) via an intermediate vector pDONR/Zeo (Life Technologies, Thermo

Fisher Scientific, USA) using standard molecular cloning techniques. The silencing constructs or control empty vector were transformed into *Agrobacterium tumefaciens* and the resulting *Agrobacterium* strains were infiltrated into *N. benthamiana* leaves at OD₆₀₀=0.4 together with *Agrobacterium* strains harboring PVA ΔHCPro (OD₆₀₀=0.05) and Fluc (OD₆₀₀=0.01). Analysis of *Renilla* and Firefly luciferase expression was carried out at 5 dpi as described previously (Eskelin *et al.* 2010).

SAMS activity measurements

N. benthamiana leaves were infiltrated with *Agrobacterium* strains harboring GUS, PVA or PVA ΔHCPro at OD₆₀₀=1. The infiltrated leaves were sampled at 5 dpi and soluble protein extracts prepared from fresh leaf tissue were immediately assayed for SAMS enzymatic activity. SAMS activity was measured as described previously (Shen *et al.*, 2002) with the following modifications: soluble protein was extracted from *N. benthamiana* leaves by homogenizing approximately 25 mg of fresh leaf tissue in 0.3 ml of pre-chilled extraction buffer (100 mM Tris-HCl (pH 7.5), 2 mM EDTA, 20% (v/v) glycerol, 20 mM β-mercaptoethanol, 1 mM DTT). After centrifugation at 10,000xg for 10 min, an aliquot of the supernatant containing approximately 60 μg of extracted protein was assayed for SAMS activity as described by Shen *et al.* (2002). Protein quantification in the supernatant was performed using a Qubit fluorometer (Life Technologies, Thermo Fisher Scientific, USA).

Immunoaffinity purification of ribosomes for LC-MS/MS analysis

Whole leaves from two independent batches of transgenic *N. benthamiana* plants expressing FLAG-tagged RPL18B were infiltrated with the *Agrobacterium* strain harboring PVA (OD₆₀₀=0.5). Similarly infiltrated non-transgenic plants were used as negative controls to account for nonspecific binding to the affinity matrix. The leaves were collected at 4 dpi for ribosome purification. Ribosomes were isolated using the previously published protocol for *A. thaliana* (Zanetti *et al.*, 2005) with several modifications. Frozen, pulverized leaf tissue (~4 ml) was mixed with one volume of polysome extraction buffer [(PEB); 200 mM Tris-HCl (pH 9.0), 200 mM KCl, 36 mM MgCl₂, 10 mM EGTA, 1 mg/ml heparin, 1 mM DTT, 50 μg/ml cycloheximide, 50 μg/ml chloramphenicol, 2% (v/v) Triton X-100, 2% (v/v) Tween 40, 2% (w/v) Brij 35, 2% (v/v) NP-40, 2% (v/v) polyoxyethylene (10) tridecyl ether and 1% (w/v) sodium deoxycholate] and incubated for 30 min at 4°C with gentle rotation. Homogenates were clarified by two consecutive centrifugations at 16,000xg for 10 min at 4°C. The supernatants were incubated with 50 μl of buffer-equilibrated

1
2
3
4
5
6
7
8
9
10
11
12
13
14
15
16
17
18
19
20
21
22
23
24
25
26
27
28
29
30
31
32
33
34
35
36
37
38
39
40
41
42
43
44
45
46
47
48
49
50
51
52
53
54
55
56
57
58
59
60

ANTI-FLAG M2 affinity gel beads (Sigma-Aldrich, USA) for 1 h at 4°C with gentle rotation. The resin was washed three times with 1 ml of wash buffer (40 mM Tris-HCl (pH 8.8), 100 mM KCl and 10 mM MgCl₂) at 4°C. The final wash was removed with an insulin syringe and ribosomes were eluted with the washing buffer containing 200 ng/μl of 3xFLAG peptide (Sigma-Aldrich, USA) for 30 min at 4°C. Eluted material was stored at -70°C.

Ribosome fractionation coupled with immunoaffinity purification

Whole leaves of transgenic *N. benthamiana* plants expressing FLAG-tagged RPL18B were infiltrated with a mixture of *Agrobacterium* strains as described in the results section (OD₆₀₀ of each strain in the mixture was 0.35). The leaves were collected at 4 dpi for ribosome fractionation. Ribosome fractionation using sucrose density gradient centrifugation was carried out as described previously (Lanet et al., 2009), except that polysome buffer contained 100 mM Tris-HCl (pH 8.8), 50 mM KCl, 25 mM MgCl₂, 5 mM EGTA, 5 mM NaF, 0.3 mg/ml heparin, 30 μg/ml cycloheximide, 30 μg/ml chloramphenicol and 0.5% (v/v) Tween 20. Fractions containing ribosomes were pooled and 300 μl aliquots were diluted 1:4.5 with polysome buffer and incubated for 1 hour at 4°C with 50 μl of ANTI-FLAG M2 affinity gel beads (Sigma-Aldrich, USA) pre-equilibrated in wash buffer (100 mM Tris-HCl (pH 8.8), 50 mM KCl, 25 mM MgCl₂, 5 mM EGTA and 5 mM NaF). After washing the beads three times with wash buffer supplemented with 0.5% (v/v) Tween 20, the final wash was removed with an insulin syringe and ribosomes were eluted with 50 μl of elution buffer (40 mM Tris-HCl (pH 8.8), 100 mM KCl and 10 mM MgCl₂) containing 200 ng/μl of 3xFLAG peptide (Sigma-Aldrich, USA) for 30 min at room temperature with shaking. Eluted material was stored at -70°C.

SDS-PAGE, silver staining and Western blotting

Proteins were separated by SDS-PAGE on precast Any kD gels (Bio-Rad Laboratories, USA). The gels were either stained with silver nitrate following the previously published protocol (Yan et al., 2000) or transferred onto Immobilon-P polyvinylidene difluoride (PVDF) membranes (Merck Millipore, USA). Prior to incubation with a primary antibody, the membranes were blocked with 3% (w/v) bovine serum albumin or 3% (w/v) skimmed milk powder in TBST buffer (50 mM Tris (pH 7.5), 150 mM NaCl, 0.1% Tween 20). Protein-antibody complexes were detected using an HRP-conjugated secondary antibody and chemiluminescent (Immobilon Western Chemiluminescent HRP Substrate, Merck Millipore, USA) or chromogenic (TMB Stabilized Substrate for HRP, Promega, USA) substrates according to the manufacturer's instructions.

RNA isolation

RNA was isolated from purified ribosome samples using RNeasy columns (Qiagen, Germany). RNA integrity was verified by agarose gel electrophoresis and ethidium bromide staining.

Supplementary References

- Eskelin, K., Hafren, A., Rantalainen, K.I., and Makinen, K.** (2011). Potyviral VPg enhances viral RNA translation and inhibits reporter mRNA translation in planta. *Journal of virology* **85**:9210-9221.
- Eskelin, K., Suntio, T., Hyvarinen, S., Hafren, A., and Makinen, K.** (2010). Renilla luciferase-based quantitation of Potato virus A infection initiated with Agrobacterium infiltration of *N. benthamiana* leaves. *Journal of virological methods* **164**:101-110.
- Lanet, E., Delannoy, E., Sormani, R., Floris, M., Brodersen, P., Crete, P., Voinnet, O., and Robaglia, C.** (2009). Biochemical evidence for translational repression by Arabidopsis microRNAs. *The Plant cell* **21**:1762-1768.
- Shen, B., Li, C., and Tarczynski, M.C.** (2002). High free-methionine and decreased lignin content result from a mutation in the Arabidopsis S-adenosyl-L-methionine synthetase 3 gene. *The Plant journal* **29**:371-380.
- Yan, J.X., Wait, R., Berkelman, T., Harry, R.A., Westbrook, J.A., Wheeler, C.H., and Dunn, M.J.** (2000). A modified silver staining protocol for visualization of proteins compatible with matrix-assisted laser desorption/ionization and electrospray ionization-mass spectrometry. *Electrophoresis* **21**:3666-3672.
- Zanetti, M.E., Chang, I.F., Gong, F., Galbraith, D.W., and Bailey-Serres, J.** (2005). Immunopurification of polyribosomal complexes of Arabidopsis for global analysis of gene expression. *Plant physiology* **138**:624-635.